NATIONAL ADVISORY COMMITTEE FOR AERONAUTICS

TECHNICAL NOTE 3917

EFFECT OF PROPELLER LOCATION AND FLAP DEFLECTION ON THE AERODYNAMIC CHARACTERISTICS OF A WING-PROPELLER COMBINATION FOR ANGLES OF ATTACK FROM 0° TO 80°

By William A. Newsom, Jr.

Langley Aeronautical Laboratory
Langley Field, Va.

Washington
January 1957

NATIONAL ADVISORY COMMITTEE FOR AERONAUTICS

TECHNICAL NOTE 3917

EFFECT OF PROPELLER LOCATION AND FLAP DEFLECTION ON THE AERODYNAMIC CHARACTERISTICS OF A WING-PROPELLER COMBINATION FOR ANGLES OF ATTACK FROM 0° TO 80°

By William A. Newsom, Jr.

SUMMARY

An investigation has been made to determine the effect of propeller location and flap deflection on the lift, drag, and pitching-moment characteristics of a wing-propeller combination over an angle-of-attack range from 0° to 80°. The model had four propellers, the slipstream from which covered practically the entire span of the wing. The wing had a 30-percent-chord slotted flap and an 8.5-percent-chord slat. Data were obtained for flap deflections of 0°, 20°, 40°, and 60° with the slat off and on. For one propeller position the power input to the model was measured and tuft studies of the flow on the wing were made. The data are analyzed to assess the feasibility, from consideration of stability and control, of a tilting-wing vertical-take-off-and-landing airplane with the wing pivoted behind the primary wing structure to provide a desirable structural configuration. The main object of the investigation was to determine whether advantage might be taken of the forward shift of the center of gravity of the airplane, as the wing is tilted from an angle of attack of 90° to 0°, to minimize the change in trim pitching moment throughout the transition speed range for such a configuration. The results indicate that with proper propeller position and programming of flap deflection, it is possible to design a configuration of this type in which essentially no change in trim is required throughout the transition from hovering to normal unstalled forward flight.

INTRODUCTION

In recent years great interest has been shown in the design of various types of airplanes for vertical take-off and landing by using either a flap arrangement to deflect the airstream downward or a tilting wing. (See, for example, refs. 1 to 3.) From consideration of the power required, the best configuration appears to be an airplane in which a combination of a

tilting wing with some flap deflection is used. With such a configuration, the use of a wing pivot well back on the wing chord to permit the use of a continuous wing structure across the top of the fuselage appears very desirable from structural and weight considerations.

In order to analyze the feasibility of a configuration employing these design features from stability and control considerations, some experimental data on the aerodynamic characteristics of an appropriate wing-propeller combination were necessary. Force tests were therefore made to determine the effect of propeller location and flap deflection on the lift, drag, and pitching-moment characteristics of a wing-propeller combination over an angle-of-attack range from 0° to 80° for flap deflections of 0°, 20°, 40°, and 60°. These data were analyzed to determine whether advantage might be taken of the forward shift of the center of gravity of the airplane, as the wing tilted from an angle of attack of 90° to 0°, to minimize the change in trim pitching moment throughout the transition-speed range for such a configuration. The investigation covered two vertical and two longitudinal positions of the propellers relative to the wing.

The results of these tests are expected to be of assistance in the design or analysis of other aircraft with similarly located propellers on a tilting wing. The data are presented with little analysis except for a brief discussion of the application of the pitching-moment results to the hypothetical vertical-take-off airplane described in reference 3.

SYMBOLS

All forces and moments are based on the wind-axis system.

F_L	lift, lb
F_D	drag, lb
M_Y	pitching moment, ft-lb
V	tunnel velocity, ft/sec
α	angle of attack of wing, deg
δ_f	angle of flap deflection, deg
$\bar{c}$	mean aerodynamic chord, 9.68 in.
P	horsepower input to model motor

APPARATUS AND TESTS

The geometric characteristics of the model used in the investigation are as follows:

Wing:	
Sweepback (0.60 chord), deg	0
Airfoil section	NACA 65-210
Aspect ratio	9
Tip chord, in.	7.11
Root chord (at center line), in.	11.85
Taper ratio	0.60
Area, sq in.	808
Span, in.	85.32
Mean aerodynamic chord, in.	9.68
Flap hinge line, percent chord	70
Propellers (four with two blades each):	
Diameter, in.	18
Solidity (each propeller)	0.079

Sketches showing the details of the model are presented in figure 1. Figure 1(a) shows the general arrangement of the model. Figure 1(b) shows the relative position of the propellers for the three configurations covered in the investigation. Figure 1(c) shows a typical airfoil section illustrating the general arrangement of the full-span slotted flap and full-span leading-edge slat.

The slat was made from 1/32-inch-thick metal sheet, had a nose section of 0.2-inch radius, a surface curved to fit the forward 8.5 percent of the wing surface, a root chord of 1 inch, and a tip chord of 0.6 inch. The nacelle fairings completely enclosed the gear boxes and their supporting brackets. Power for the two-blade propeller mounted on each gear box was supplied through connecting shafts by a 5-horsepower electric motor which was mounted at the midspan of the wing. The propellers were the same as those used in the investigation reported in reference 1. The model was made up of components available from other investigations made at the Langley Laboratory; it was therefore necessary that the shafts between the motor and gear boxes be externally mounted but because of their relatively small size, their effect on the lift, drag, and pitching moment at the high angles of attack of primary interest was considered to be negligible.

The force tests were made in the Langley free-flight tunnel, which has a 12-foot octagonal test section. Tests were made for the three propeller locations shown in figure 1(b), which, for convenience, are called the lower rear, lower forward, and upper forward positions. For each propeller position the slotted flap was set at angles of 0°, 20°, 40°,

and 60° and an angle-of-attack range of 0° to 80° was run for each flap setting. At each angle of attack the tunnel speed was varied so that readings of the lift, drag, and pitching moment were obtained at speeds both above and below the drag trim speed. Tests were not run for angles of attack above 70° except at $\delta_f = 0°$ because the tunnel speed was approaching zero and the drag trim points were unobtainable. All tests were made at a propeller speed of 3,000 rpm. The lift, drag, and pitching moments were measured on an electric strain-gage balance which was located below the wing immediately behind the model motor.

In order to provide some indication of the variation of power required with speed, flap deflection, and slat deflection, the power input to the model motor was measured with a polyphase wattmeter. These power measurements were made for the configuration of the upper forward propeller location at the speeds corresponding to zero drag for the four flap deflections with slat on and off. At the same time that these power tests were being made, a study of the flow patterns on the wing was made by using rows of tufts taped on the upper surface of the wing. Sketches were made of the type of flow over various sections of the wing throughout the angle-of-attack range for all four flap positions.

RESULTS AND DISCUSSION

Basic Data

The lift, drag, and pitching-moment characteristics of the model obtained from the force tests throughout the speed and angle-of-attack range are presented in figures 2 to 4 as follows:

Nacelle position	δ_f, deg	Slat	Figure
Lower rear	0	Off	2(a)
	20	Off	2(b)
	40	Off	2(c)
	40	On	2(d)
	60	Off	2(e)
	60	On	2(f)
Lower forward	0	Off	3(a)
	0	On	3(b)
	20	Off	3(c)
	20	On	3(d)
	40	Off	3(e)
	40	On	3(f)
	60	Off	3(g)
	60	On	3(h)

Nacelle position	δ_f, deg	Slat	Figure
Upper forward	0	Off	4(a)
	0	On	4(b)
	20	Off	4(c)
	20	On	4(d)
	40	Off	4(e)
	40	On	4(f)
	60	Off	4(g)
	60	On	4(h)

These results are presented in dimensional terms because the conventional coefficients become inadequate when the free-stream velocity is zero. The pitching moments in these data are referred to the quarter-chord point of the mean aerodynamic chord.

The data obtained in the power input tests were scaled up to an arbitrarily chosen constant lift of 25 pounds as follows: At each drag trim point a factor was determined that would bring the measured lift up to 25 pounds. The measured power input was then scaled up by applying the factor raised to the 3/2 power and the corresponding velocity was scaled up by using the square root of the factor. The results of the tests were then plotted and are presented in figure 5. It may be seen that initially the maximum power required is for $V = 0$ or hovering condition and that the power needed for steady level flight decreases with increasing forward speed up to speeds of approximately 40 to 50 feet per second. The power required then increases again as the speed is increased further. Deflecting the flap to 40° reduces the power required as was expected from previous data (ref. 3). The use of the slat generally caused only a very small reduction in the power required.

The results of the tuft studies that were made at the speed required for zero drag at each angle of attack and flap setting are presented in figure 6. The data show that without the slat the wing experienced almost complete stall in some conditions. With the slat on, however, no areas of completely stalled flow were observed although in some cases very large areas of disturbed flow remained. The tuft studies also indicate the most consistently smooth flow area is at the wing tips and the most consistently stalled area is between the nacelles. This characteristic is believed to be due to the direction of rotation of the propellers since the blade motion is downward in the region of the wing tips and upward in the region between the nacelles (fig. 1(a)). Inasmuch as the model motor in this configuration came above the upper surface of the wing at midspan, the flow was turbulent rather than smooth, as would be expected from this propeller effect.

The reason for making the tests with a slat was to determine whether it could reduce the intensity of the stall and thereby give a reduction

in the power required at low forward speeds. Since the data show no appreciable reduction in power required, even though they do show that the slat reduced the intensity of the stall, the use of the slat does not appear very promising on the basis of the present data. It should be realized, however, that the power-required tests were made at zero drag and in the conditions required in descending flight at low speed, the slat might be very desirable. A different slat position may also give better results. These points are brought out in the data of reference 4.

Application of Data

As pointed out previously, the tests were made to provide data with which to analyze the feasibility, from consideration of stability and control, of designing a structurally desirable tilting-wing vertical-take-off airplane with the wing pivot behind the primary wing structure. Because in this configuration the airplane center of gravity would shift forward as the wing tilted from α of 90° to 0°, the main object of the investigation was to determine whether this shift in the center of gravity could be used to minimize the change in trim pitching moment throughout the transition speed range. With this object in mind, the data have been analyzed for the hypothetical vertical-take-off airplane discussed in reference 3. The assumed airplane characteristics are as follows:

Normal gross weight, lb	60,000
Empty weight, lb	41,000
Propeller diameter, ft	20
Engine power (four engines), bhp	3,500
Tail-engine thrust (two engines), lb	1,800
Wing area, sq ft	1,000
Wing span, ft	95

A sketch of this airplane is reproduced in figure 7.

For this analysis, pitching moments were transferred to the center-of-gravity positions of the complete airplane configuration, which varied with wing incidence and were different for each of the three propeller positions covered in the tests. Figure 8 shows the center-of-gravity positions for each of the three propeller positions at 0° and 90° wing incidence as determined by the following procedure. A weight breakdown for the airplane indicated that, of the total weight of 60,000 pounds, 27,675 pounds was the weight of the tilting part of the airplane or wing group (wing, nacelles, propellers, gearing, shafting, fuel, etc.), and 32, 325 pounds was the weight of the fixed part of the airplane (fuselage, tails, landing gear, crew, cargo, etc.). The wing was assumed to be pivoted at the 65-percent point of the root chord and the wing was placed on the fuselage so that, when the wing was in the vertical position, the center of gravity

of the complete airplane would fall on the thrust line as shown in figure 8. As the wing pivoted forward for normal flight, its center of gravity moved forward and downward so that the center of gravity of the complete airplane also moved forward and downward in an arc. The pitching moments were computed with reference to this moving center of gravity of the airplane and are presented in figure 9.

It can be seen that the pitching moments obtained at the two lower propeller positions are not very different from each other at corresponding angles of attack and flap deflection but changed considerably when the propellers were moved to the upper position. In general, the plots show that for the lower positions the pitching moments are nose down (M_Y negative) throughout most of the angle-of-attack range (figs. 9(a) and 9(b)) but for the upper position (fig. 9(c)) the pitching moments are nose up throughout most of the angle-of-attack range. The fact that the upper propeller position does not give larger nose-down moments than the lower position is contrary to the result that might be expected from a first analysis of the relation between the thrust line and the center of gravity. This effect of vertical propeller position is probably caused by a difference in the forward shift of the thrust line on the propeller disk with forward speed. This forward shift of the thrust vector on the propeller disk is discussed in reference 5, which presents data for an isolated propeller and a propeller in the presence of a wing.

Since pitching moment that must be trimmed out by an auxiliary tail jet or some other device should be as small as possible, it appears that a propeller position somewhere between the lower position, which gives a nose-down moment, and the upper position, which gives a nose-up moment, would be an optimum position at which the pitching moments throughout the transition range would be close to zero. Another technique that could be used to help eliminate a variation of pitching moment during the transition period would be a careful programming of the flap deflection. As an example of the possibilities of these techniques, the data from figures 9(b) and 9(c) were interpolated to represent the results that might be obtained from an optimumized propeller position two-thirds of the distance from the upper to the lower propeller position and from a program of flap angles selected to give a nearly zero pitching moment until the forward speed had become great enough to permit the tail to be an effective trimming device. These data are presented in figure 10. The presence of a tail on a complete airplane configuration will modify these results quantitatively, and the data presented here should not be interpreted as defining an optimum configuration.

CONCLUDING REMARKS

The results of the present investigation of a wing-propeller combination show the existence of powerful factors for changing the variation of pitching moment with speed. An analysis of the data for one arbitrarily chosen case of a tilting-wing vertical-take-off-and-landing airplane indicates that with proper propeller position and programming of flap deflection, it is possible to design a configuration for a vertical-take-off-and-landing airplane in which essentially no change in trim is required throughout the transition from hovering to normal unstalled forward flight.

Langley Aeronautical Laboratory,
National Advisory Committee for Aeronautics,
Langley Field, Va., October 24, 1956.

REFERENCES

1. Tosti, Louis P., and Davenport, Edwin E.: Hovering Flight Tests of a Four-Engine-Transport Vertical Take-Off Airplane Model Utilizing a Large Flap and Extensible Vanes for Redirecting the Propeller Slipstream. NACA TN 3440, 1955.

2. Lovell, Powell M., Jr., and Parlett, Lysle P.: Hovering-Flight Tests of a Model of a Transport Vertical-Take-Off Airplane With Tilting Wing and Propellers. NACA TN 3630, 1956.

3. McKinney, M. O., Kuhn, R. E., and Hammack, J. B.: Problems in the Design of Propeller-Driven Vertical Take-Off Transport Airplanes. Aero. Eng. Rev., vol. 15, no. 4, Apr. 1956, pp. 68-75, 84.

4. Kuhn, Richard E., and Hayes, William C., Jr.: Wind-Tunnel Investigation of Effect of Propeller Slipstreams on Aerodynamic Characteristics of a Wing Equipped With a 50-Percent-Chord Sliding Flap and a 30-Percent-Chord Slotted Flap. NACA TN 3918, 1957.

5. Kuhn, Richard E., and Draper, John W.: Investigation of the Aerodynamic Characteristics of a Model Wing-Propeller Combination and of the Wing and Propeller Separately at Angles of Attack Up to 90°. NACA Rep. 1263, 1956. (Supersedes NACA TN 3304 by Draper and Kuhn.)

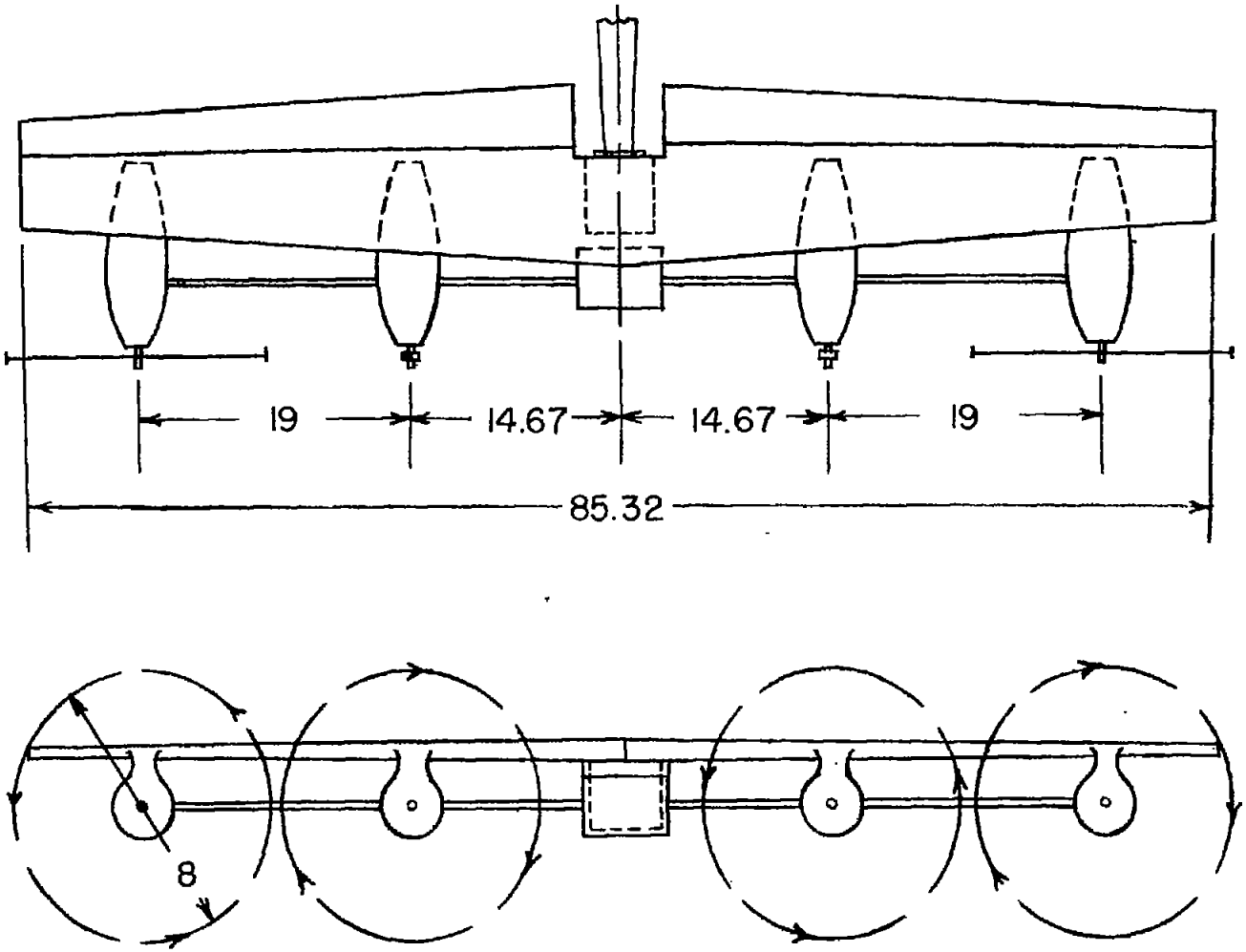

(a) Complete model shown with propellers in the lower forward position. All dimensions are in inches.

Figure 1.- Model of wing-propeller combination.

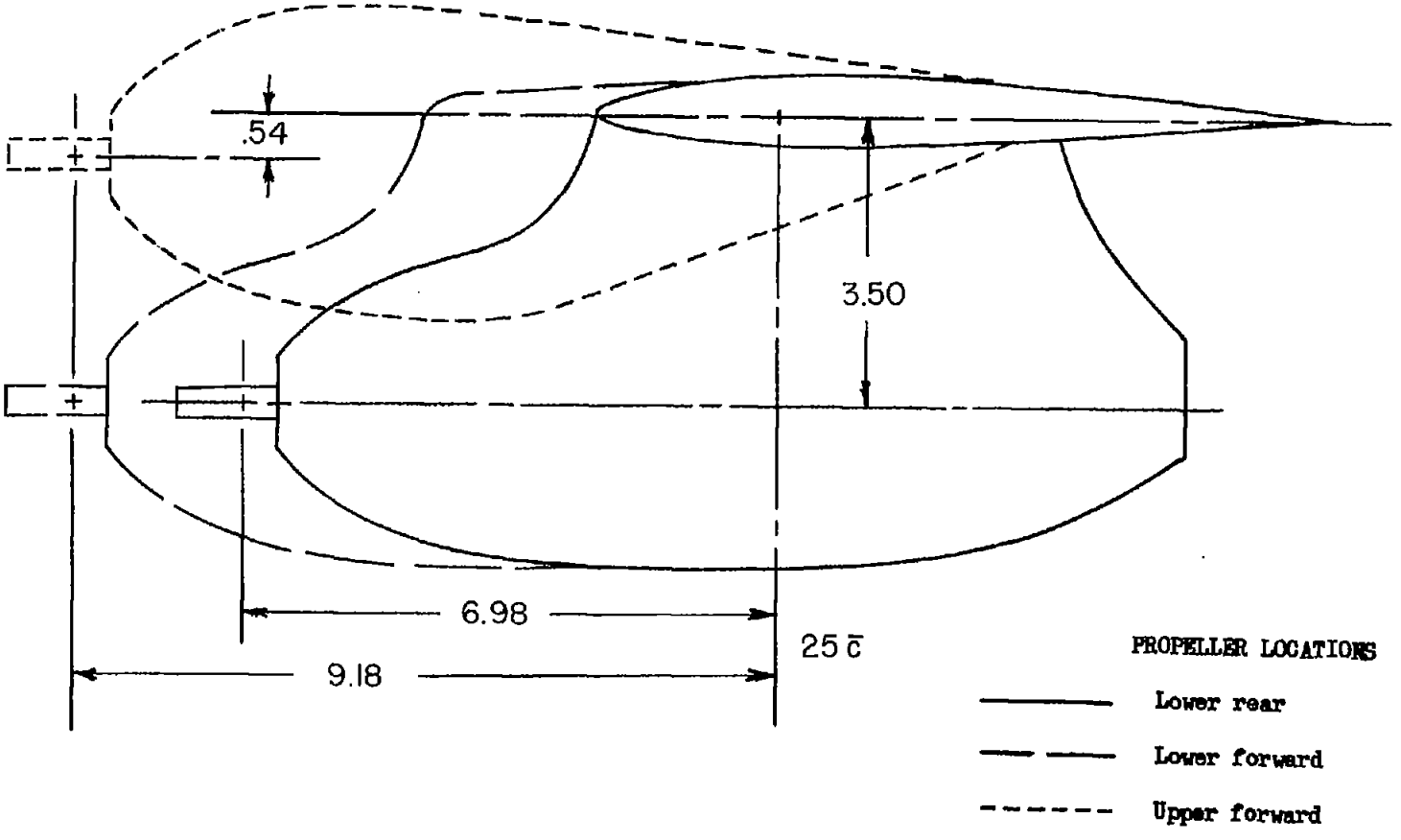

(b) Relative locations of the three propeller configurations tested. All dimensions are in inches.

Figure 1.- Continued.

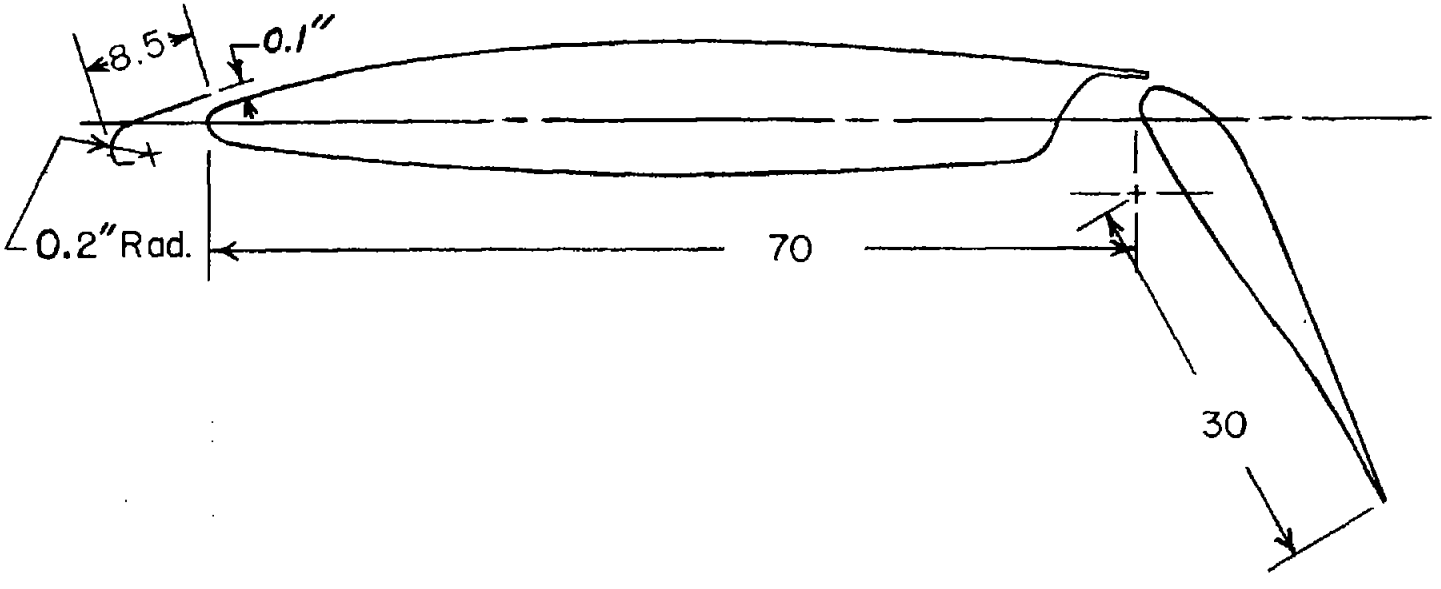

(c) Typical wing section showing flap and slat details. Flap at 60°. All dimensions in percent chord except as shown.

Figure 1.- Concluded.

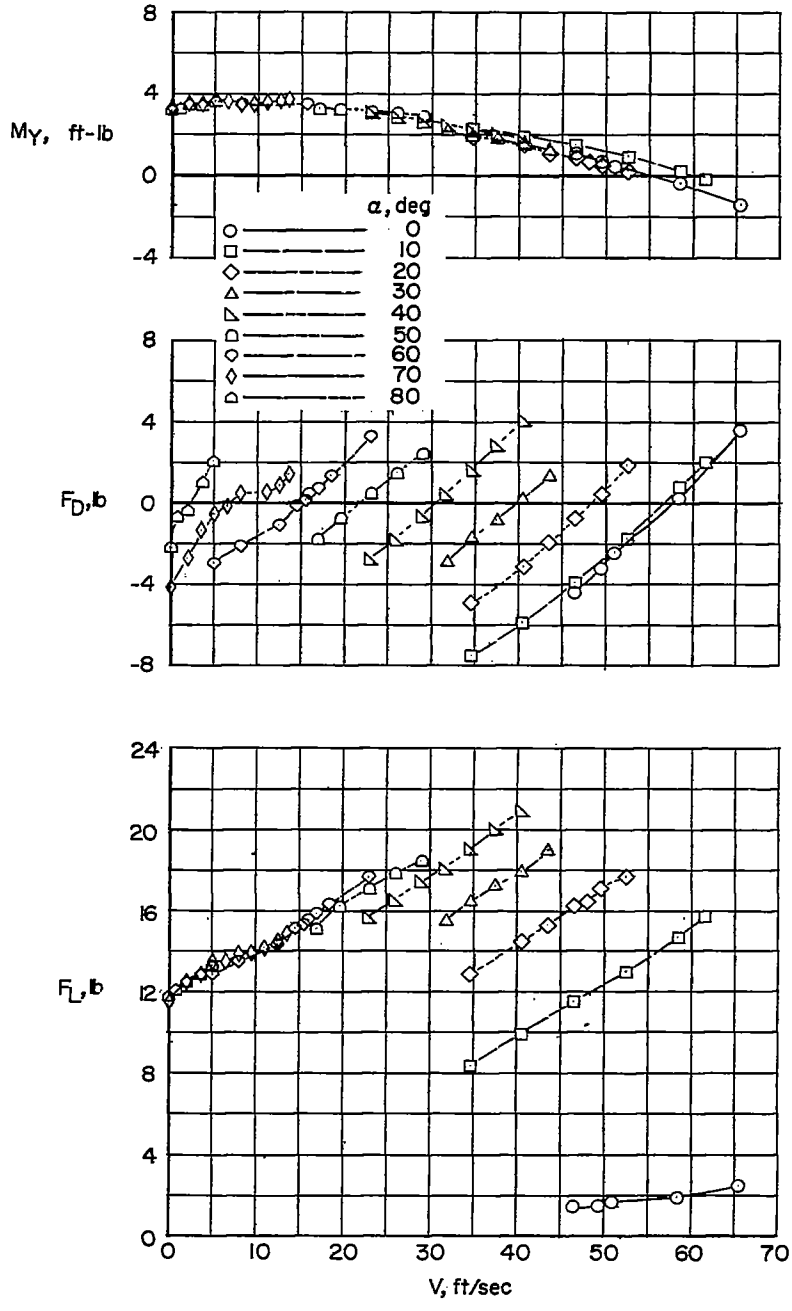

(a) $\delta_f = 0°$; slat off.

Figure 2.- Variation of lift, drag, and pitching moment with airspeed. Lower rear propeller location, pitching moment referred to $0.25\bar{c}$.

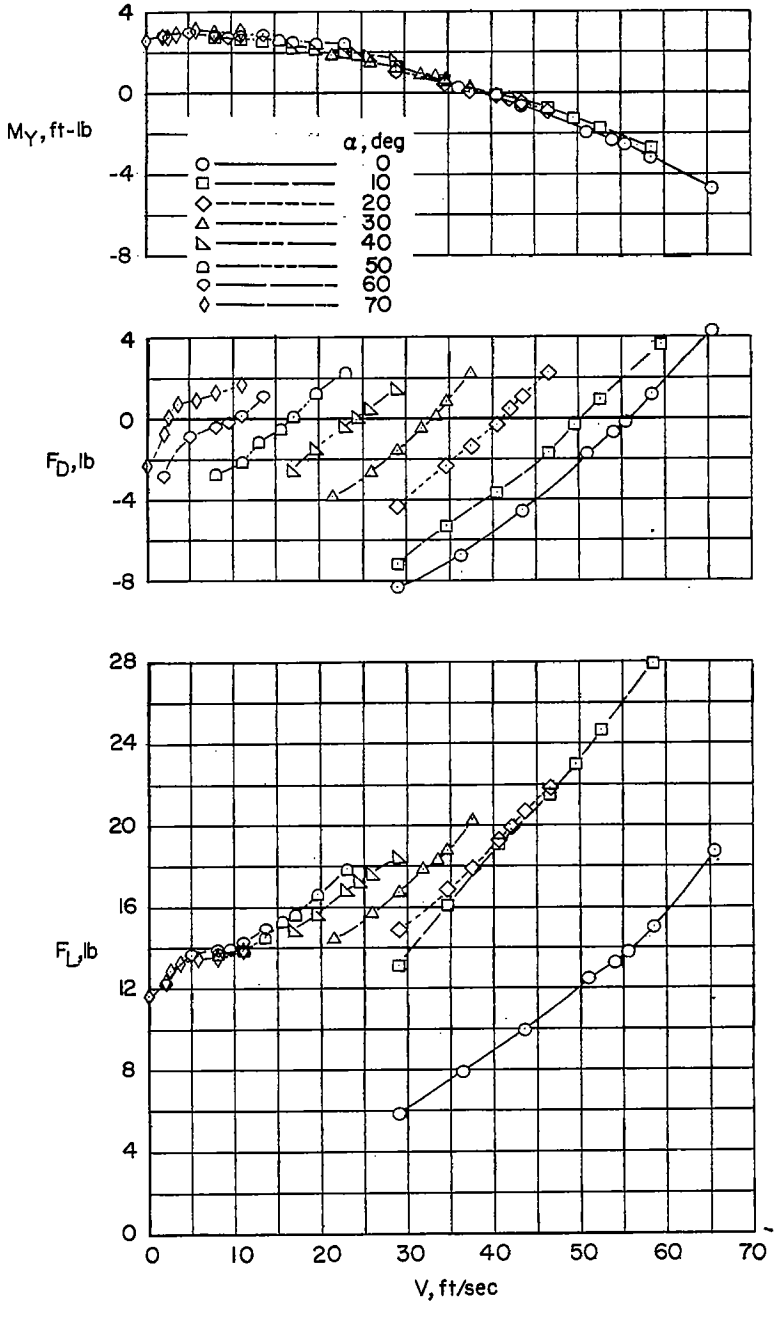

(b) $\delta_f = 20^\circ$; slat off.

Figure 2.- Continued.

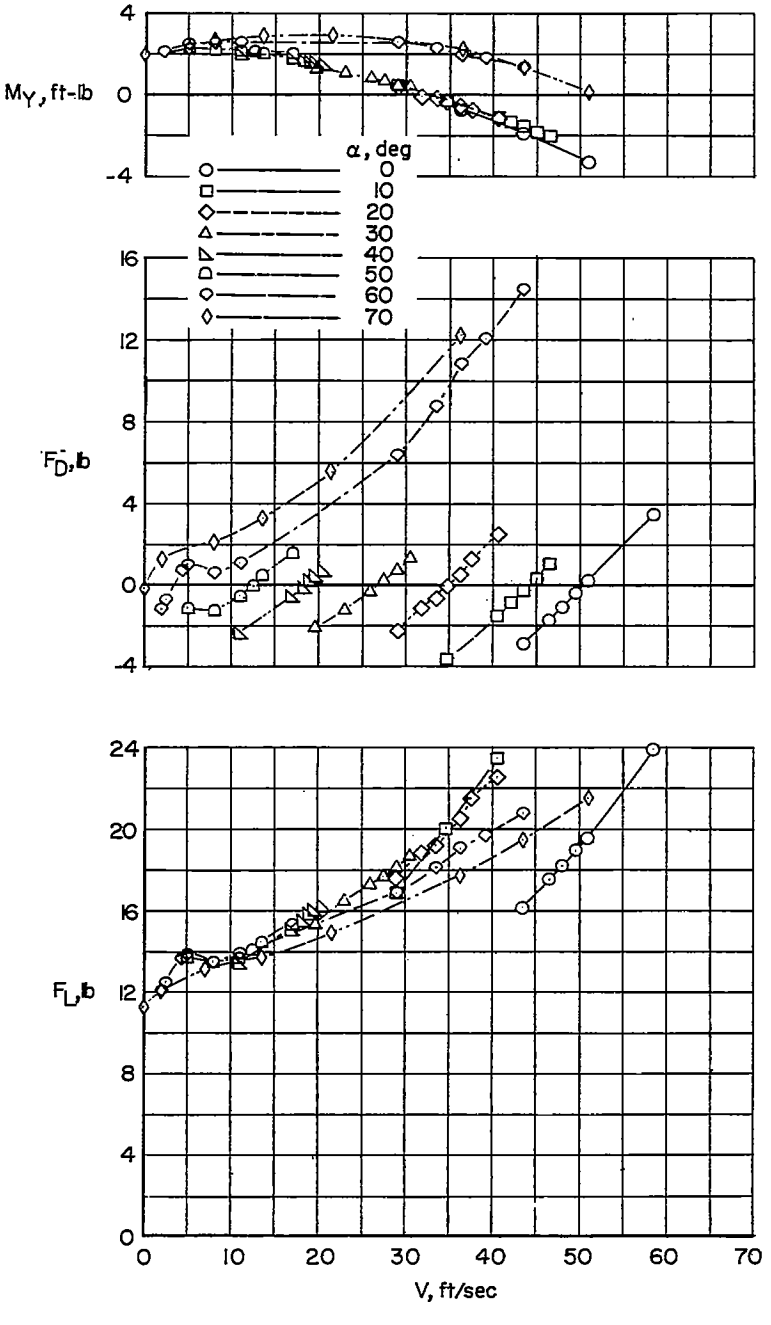

(c) $\delta_f = 40°$; slat off.

Figure 2.- Continued.

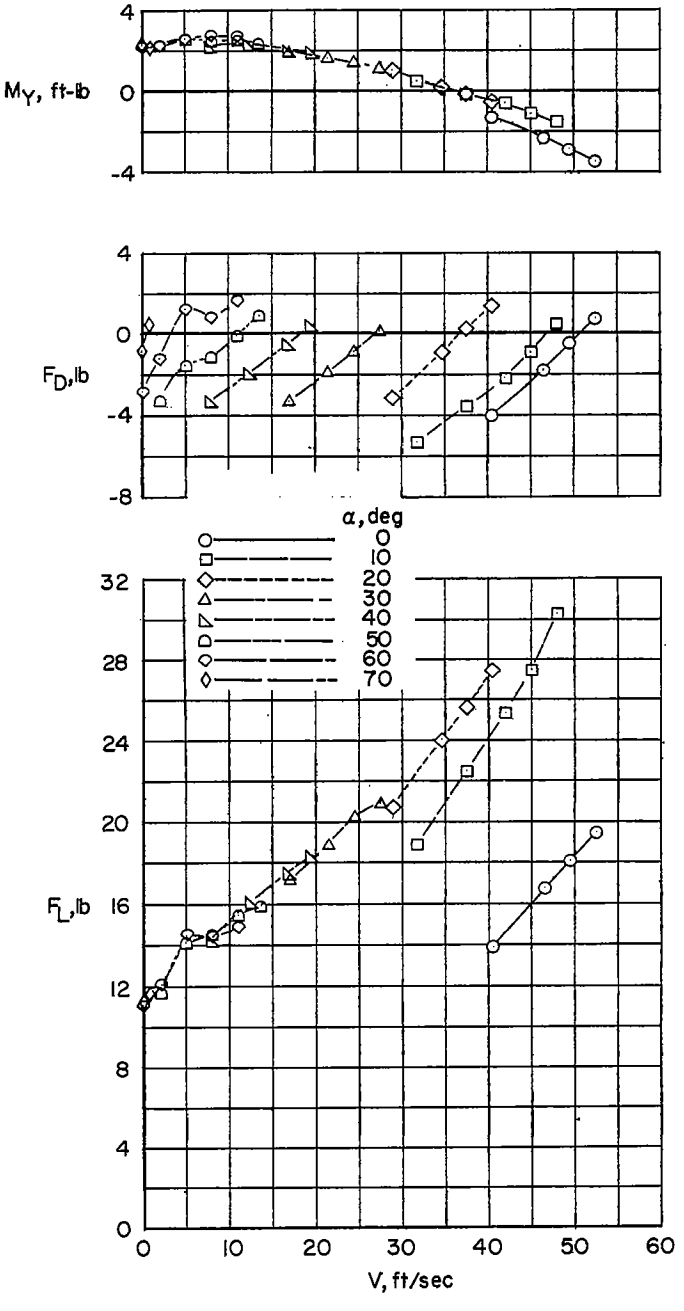

(d) $\delta_f = 40°$; slat on.

Figure 2.- Continued.

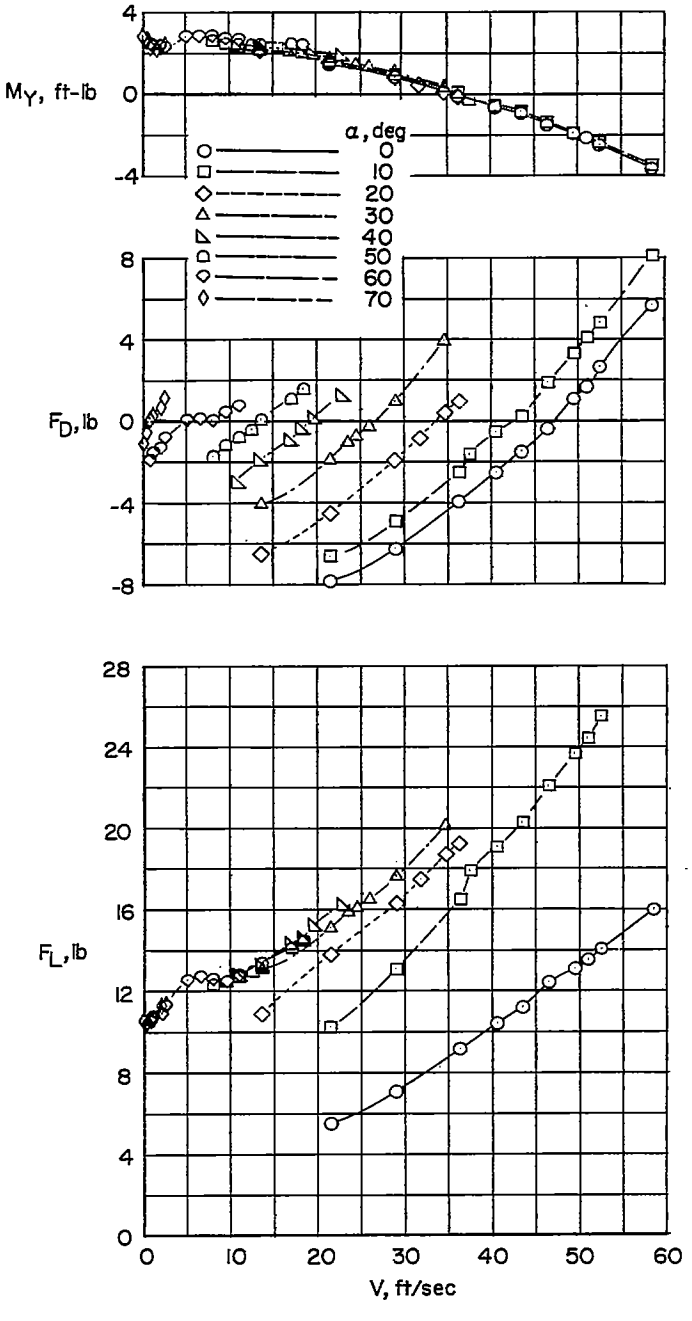

(e) $\delta_f = 60^\circ$; slat off.

Figure 2.- Continued.

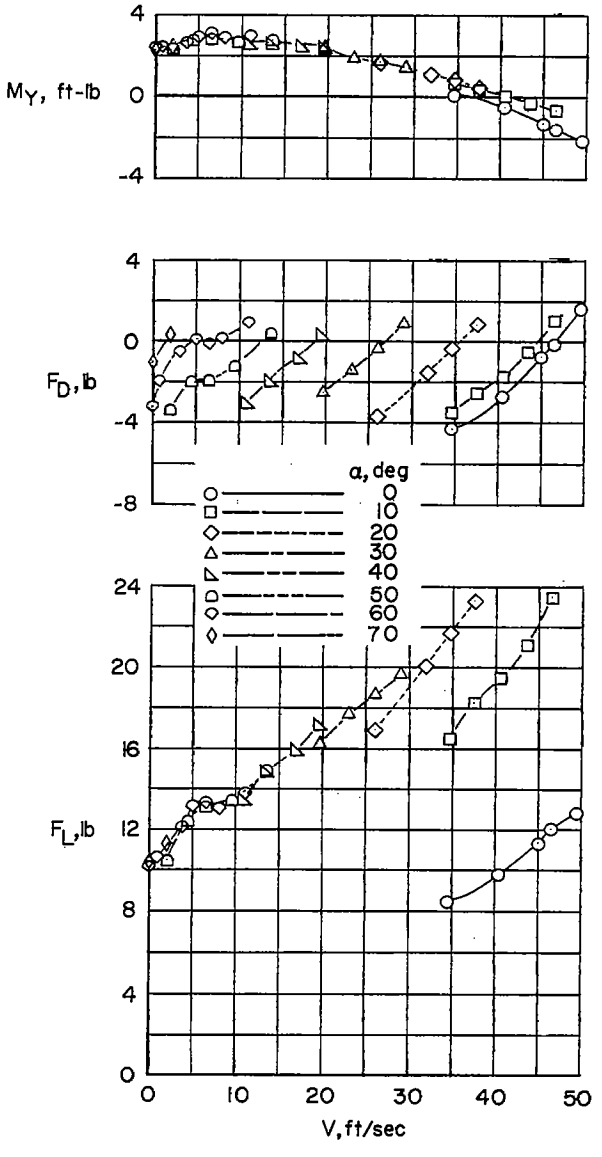

(f) $\delta_f = 60°$; slat on.

Figure 2.- Concluded.

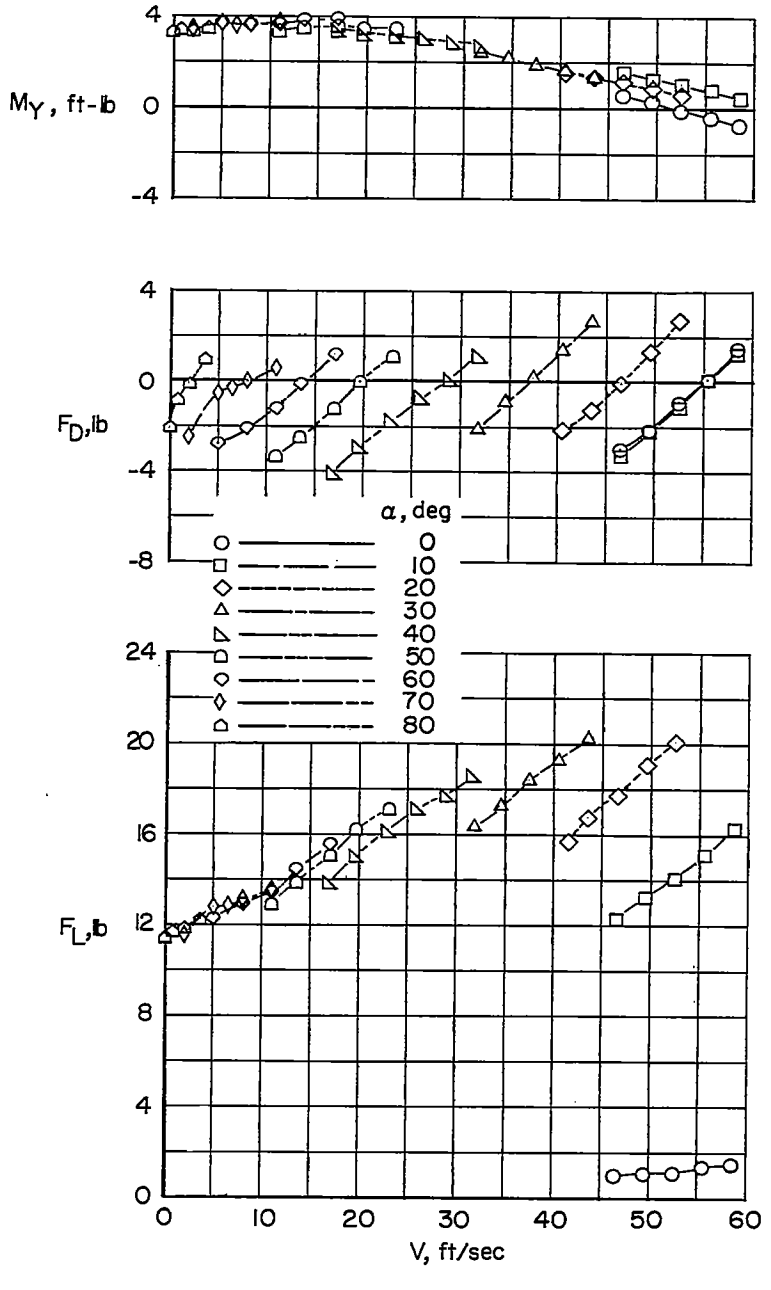

(a) $\delta_f = 0°$; slat off.

Figure 3.- Variation of lift, drag and pitching moment with airspeed. Lower forward propeller location, pitching moment referred to 0.25$\bar{c}$.

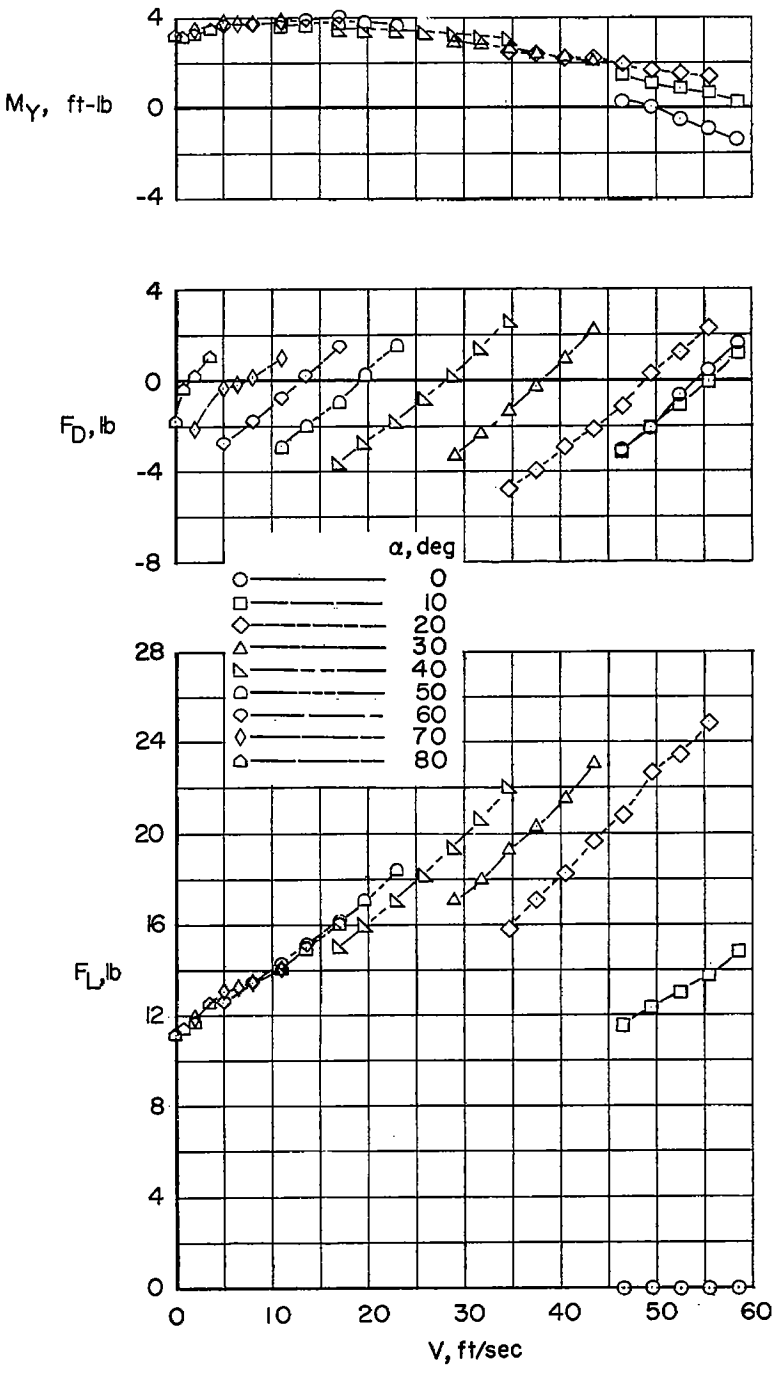

(b) $\delta_f = 0^\circ$; slat on.

Figure 3.- Continued.

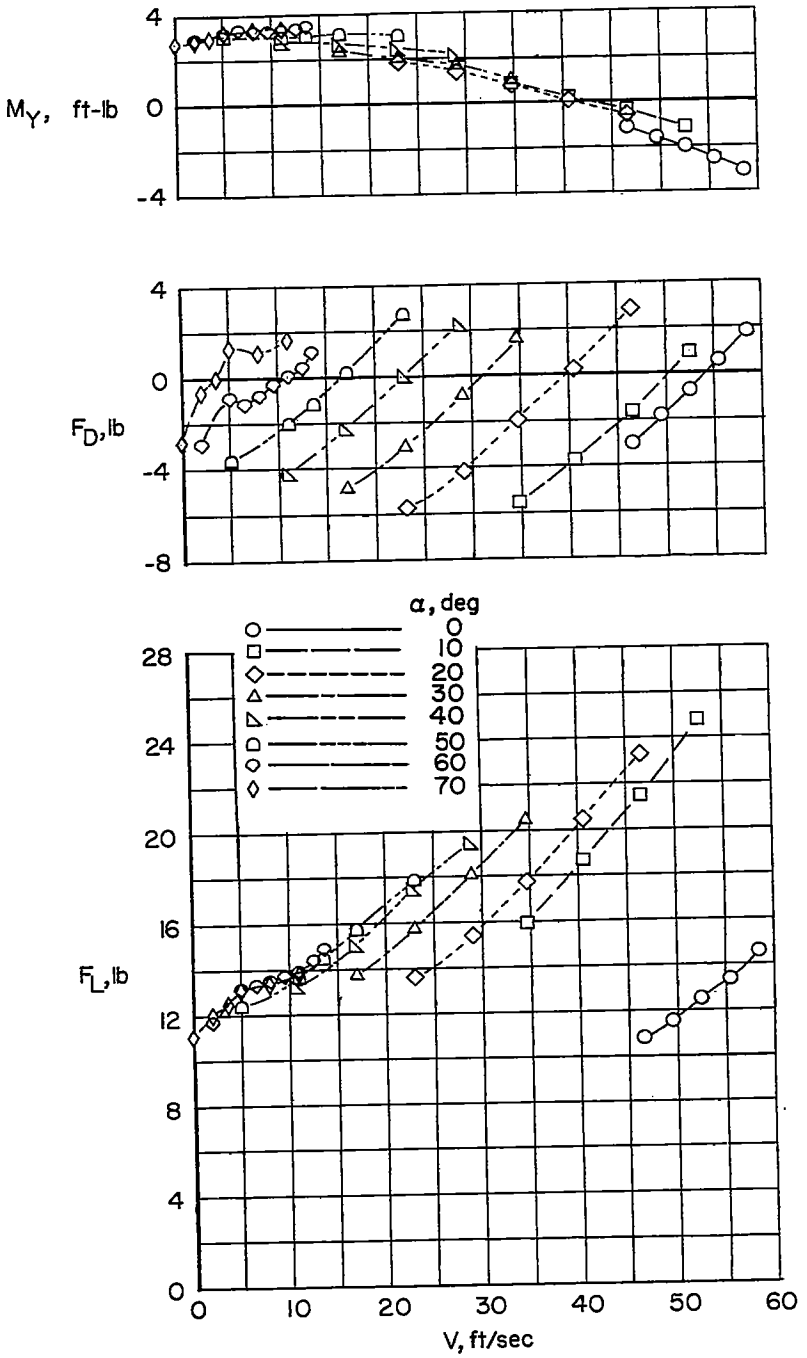

(c) $\delta_f = 20^\circ$; slat off.

Figure 3.- Continued.

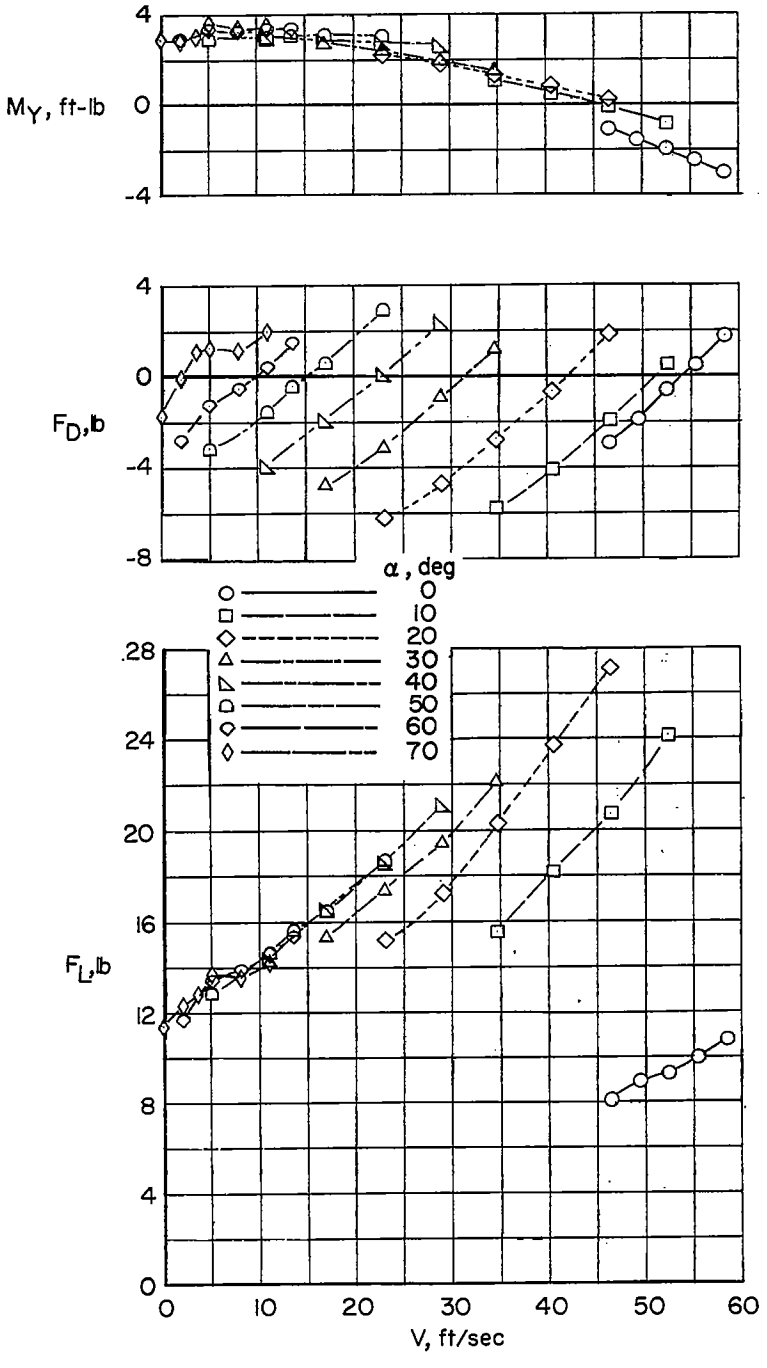

(d) $\delta_f = 20^\circ$; slat on.

Figure 3.- Continued.

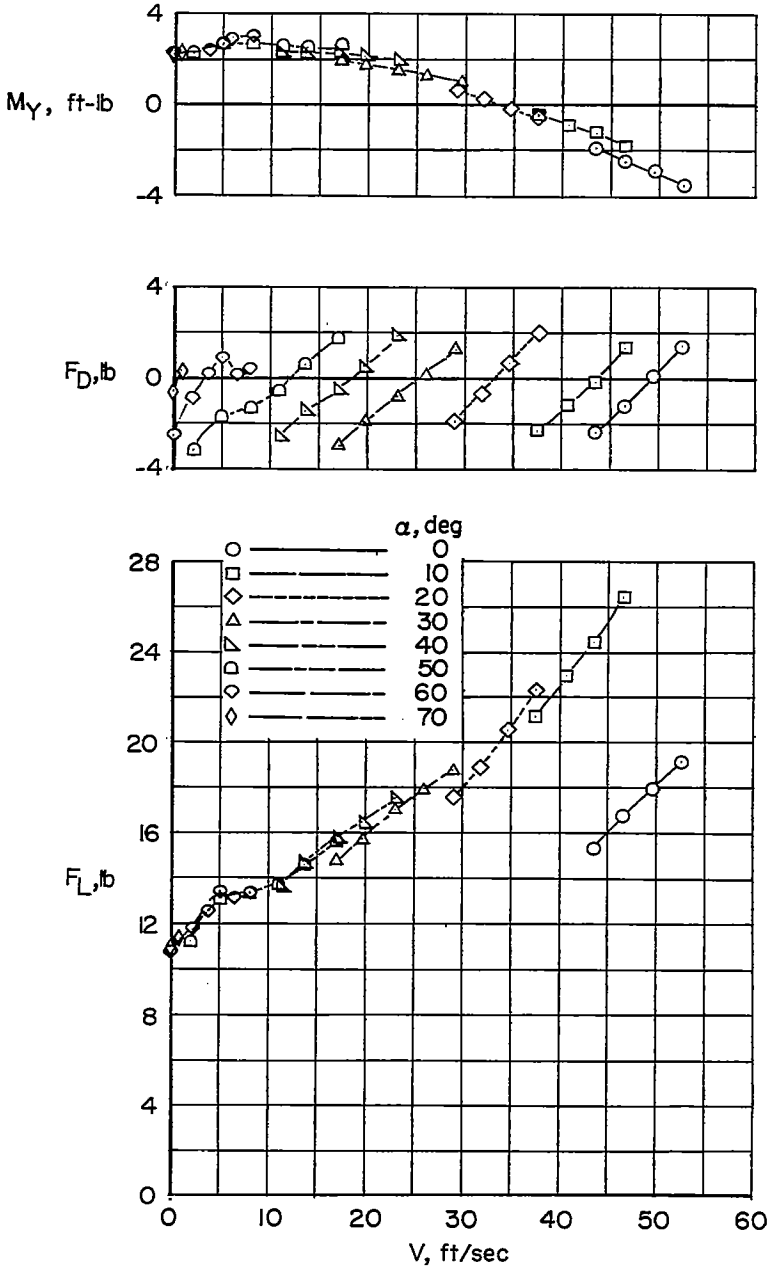

(e) $\delta_f = 40^\circ$; slat off.

Figure 3.- Continued.

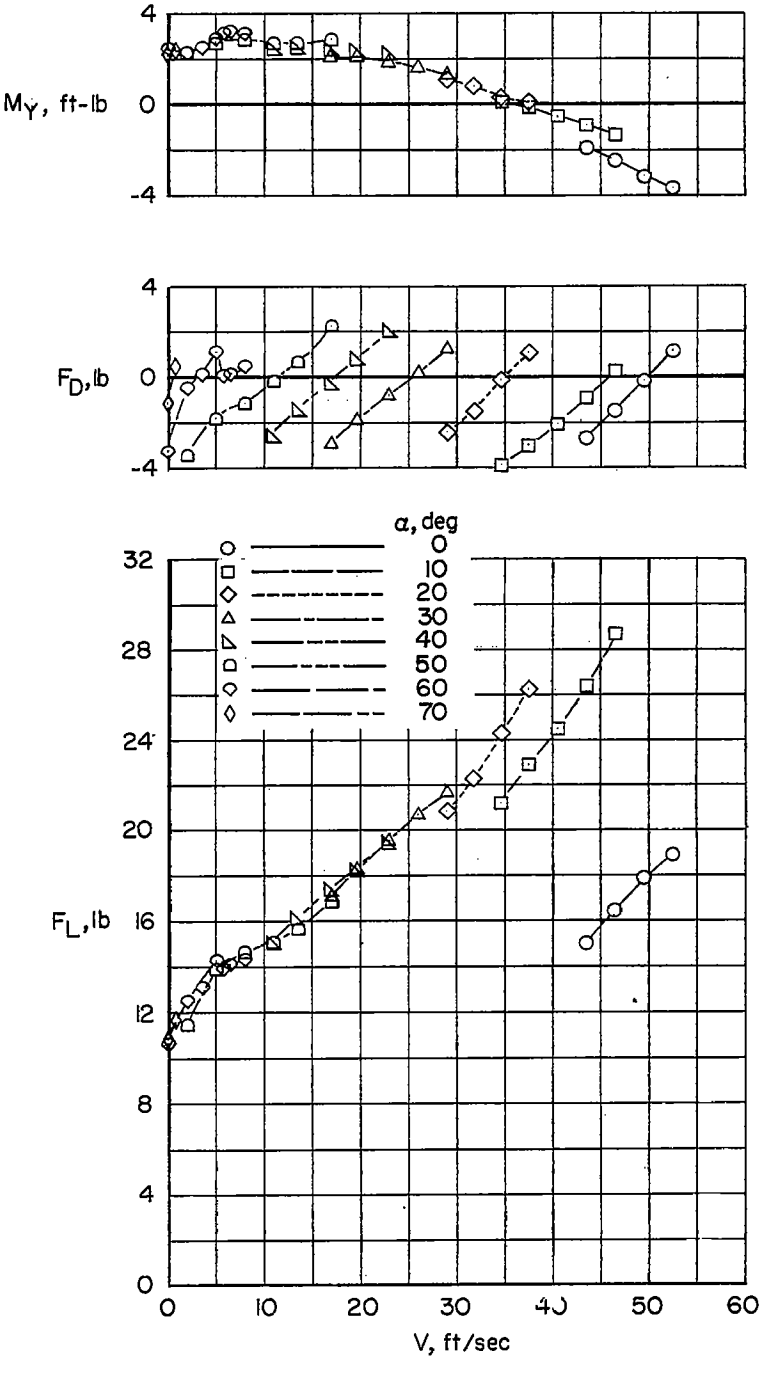

(f) $\delta_f = 40^\circ$; slat on.

Figure 3.- Continued.

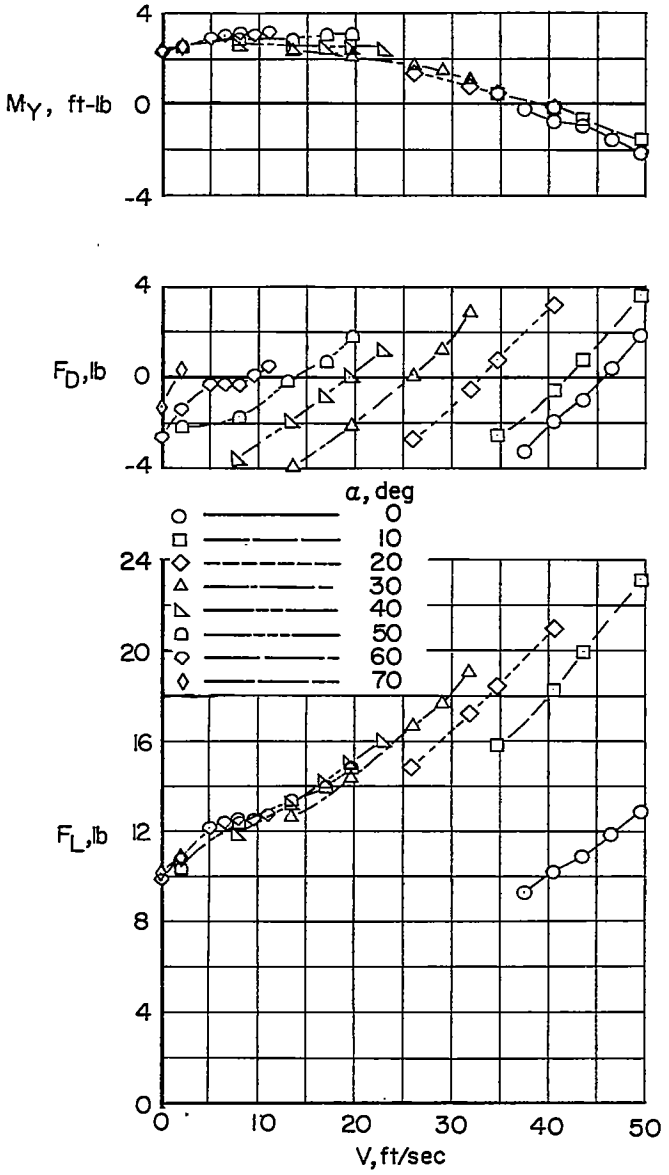

(g) $\delta_f = 60°$; slat off.

Figure 3.- Continued.

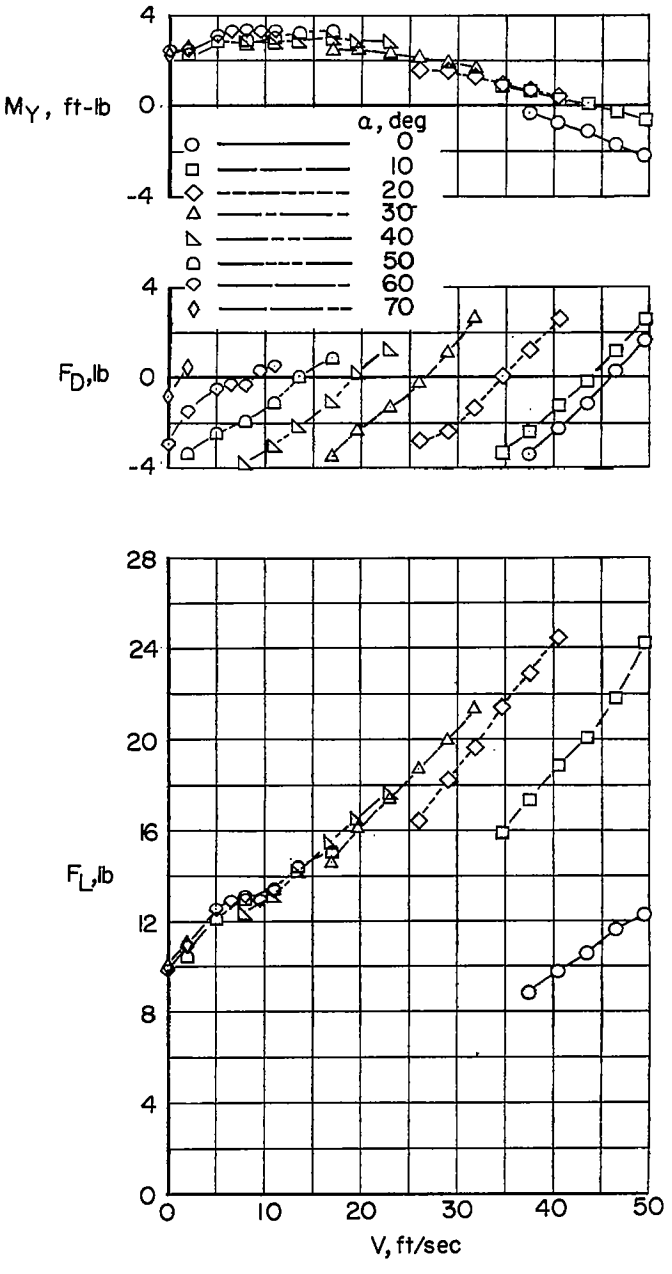

(h) $\delta_f = 60^\circ$; slat on.

Figure 3.- Concluded.

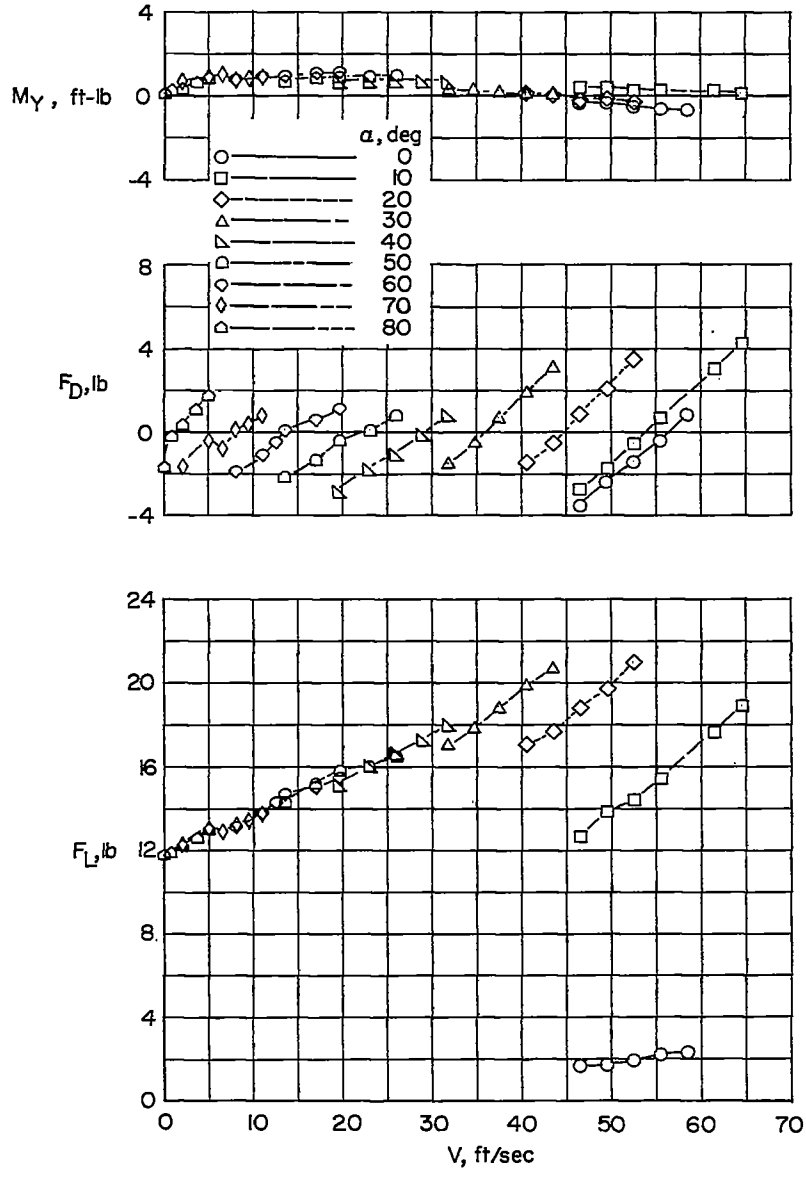

(a) $\delta_f = 0°$; slat off.

Figure 4.- Variation of lift, drag, and pitching moment with airspeed. Upper forward propeller location, pitching moment referred to 0.25$\bar{c}$.

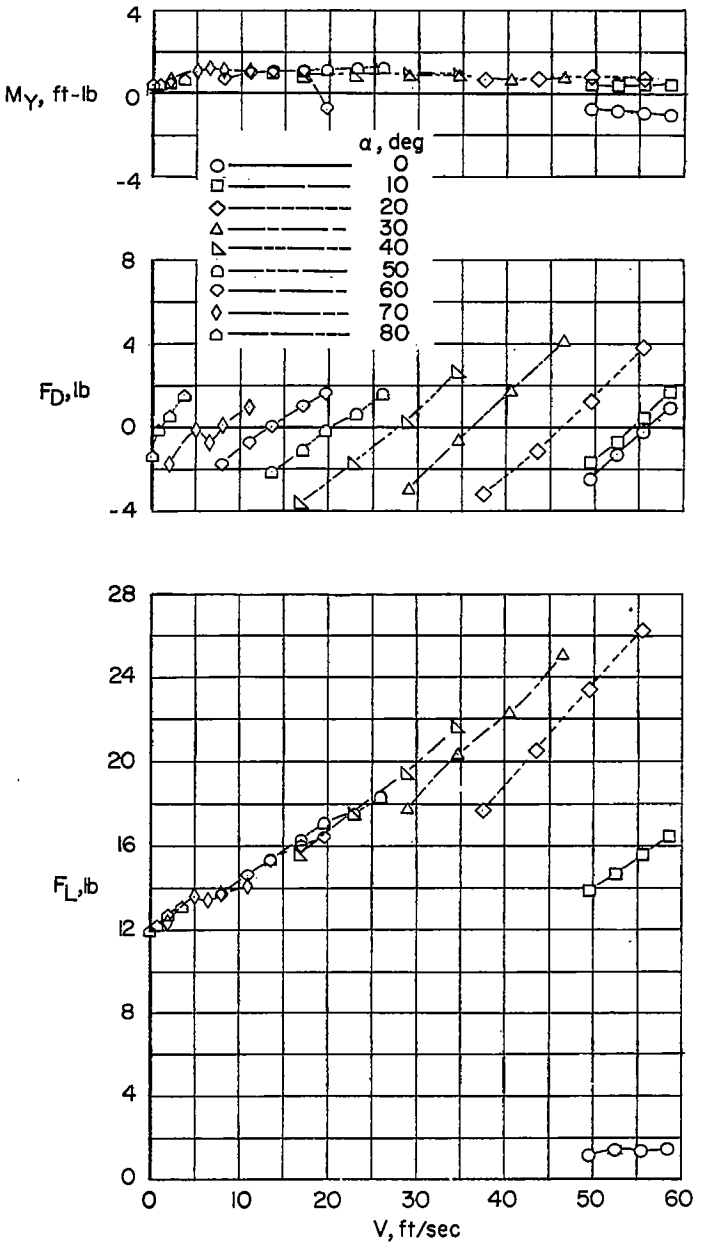

(b) $\delta_f = 0^\circ$; slat on.

Figure 4.- Continued.

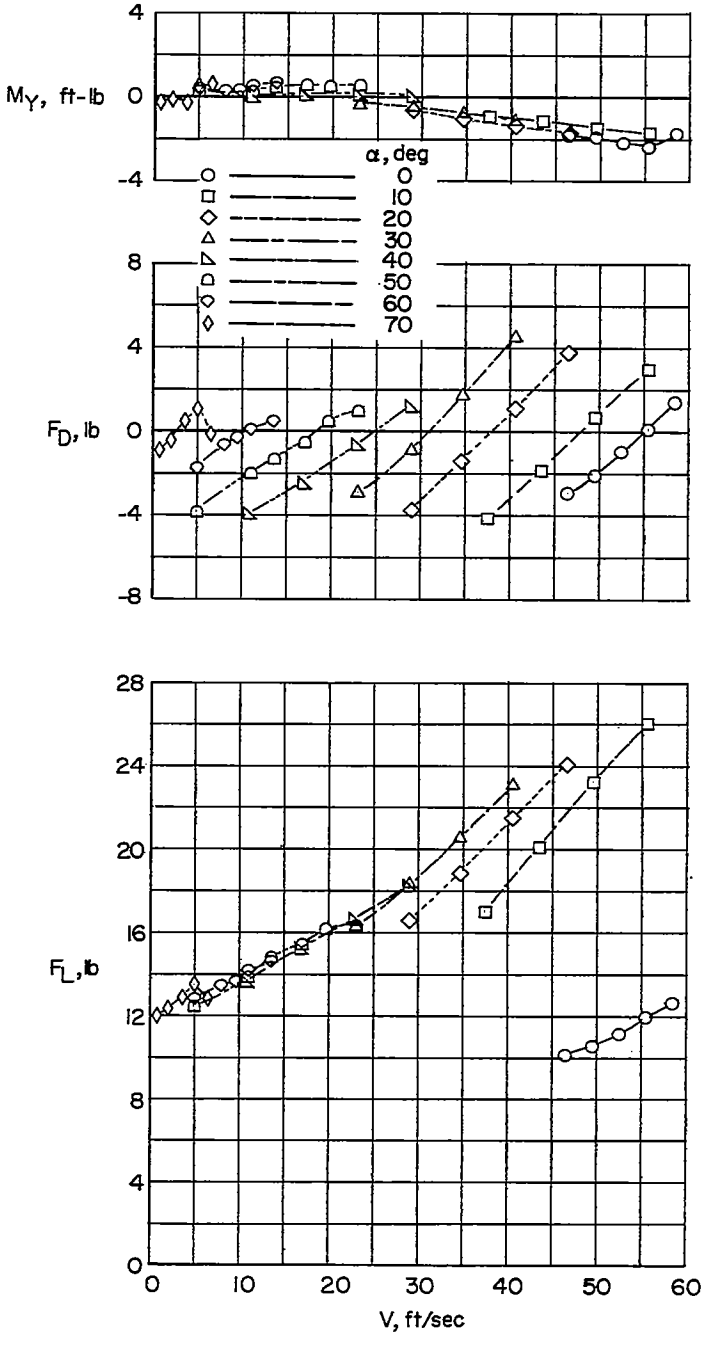

(c) $\delta_f = 20^\circ$; slat off.

Figure 4.- Continued.

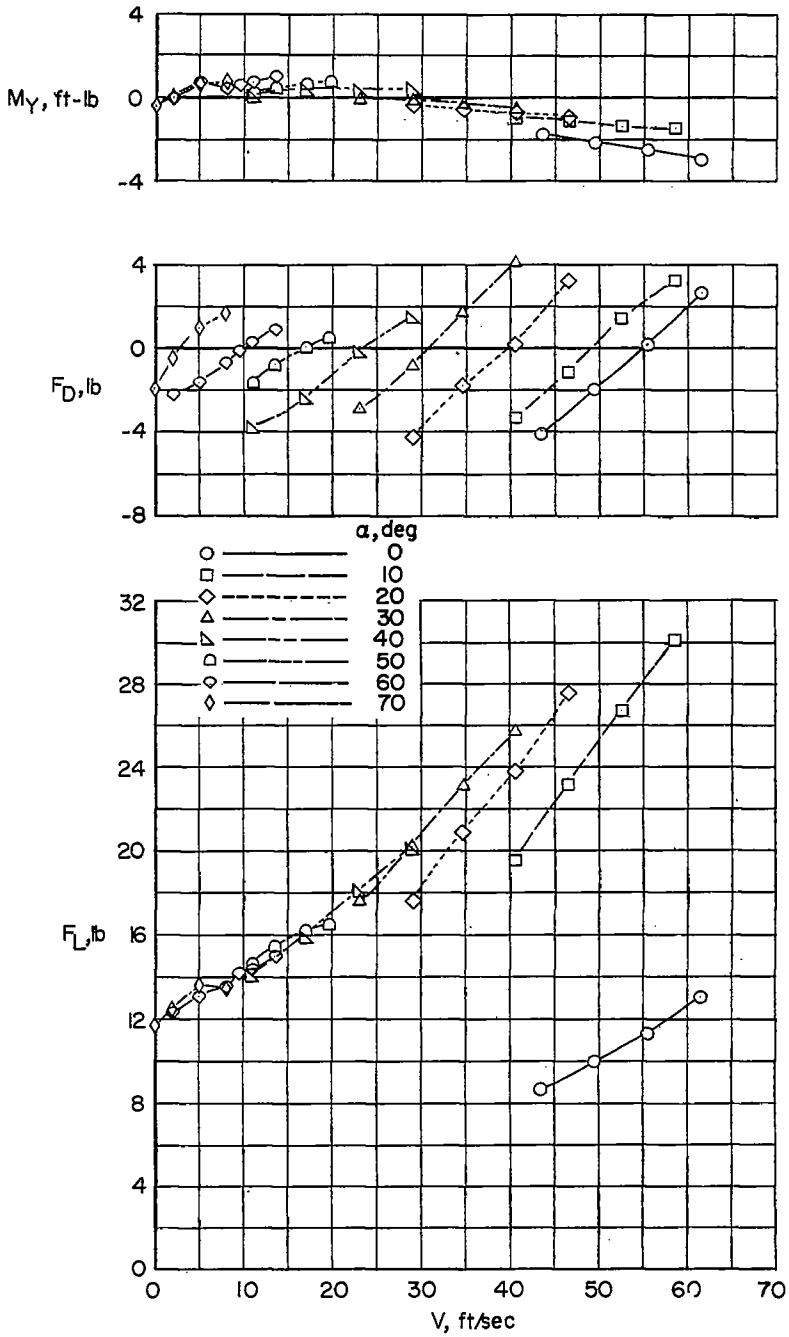

(d) $\delta_f = 20^\circ$; slat on.

Figure 4.- Continued.

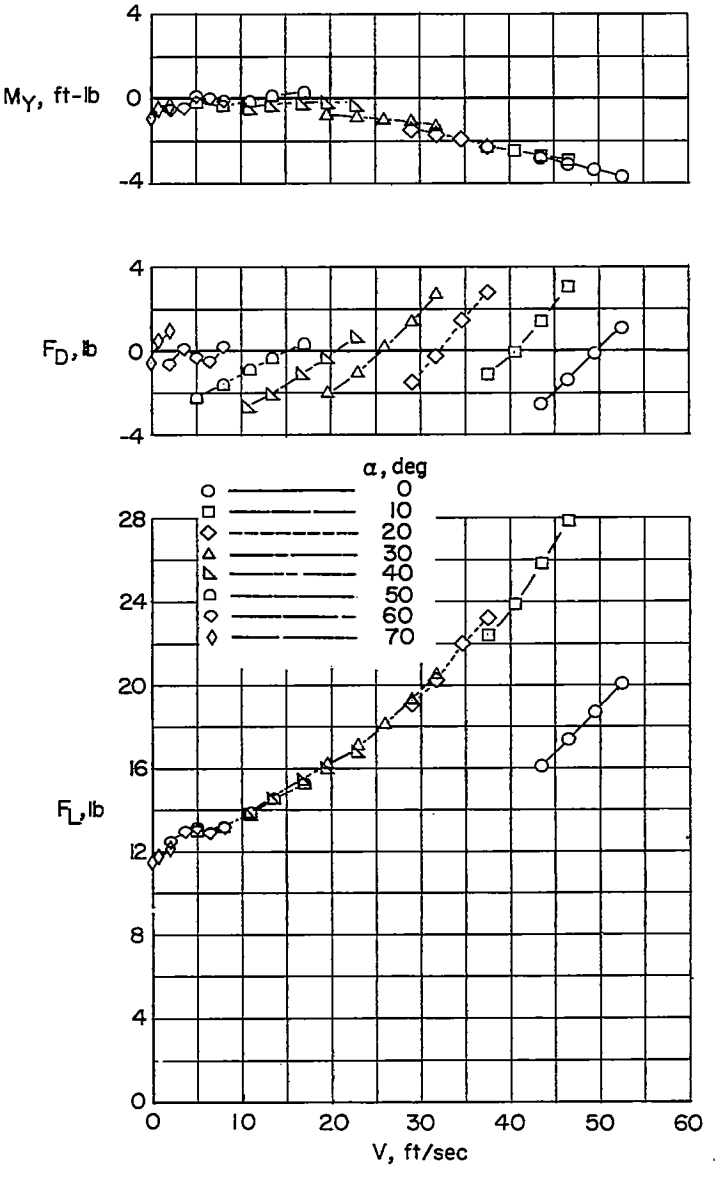

(e) $\delta_f = 40^\circ$; slat off.

Figure 4.- Continued.

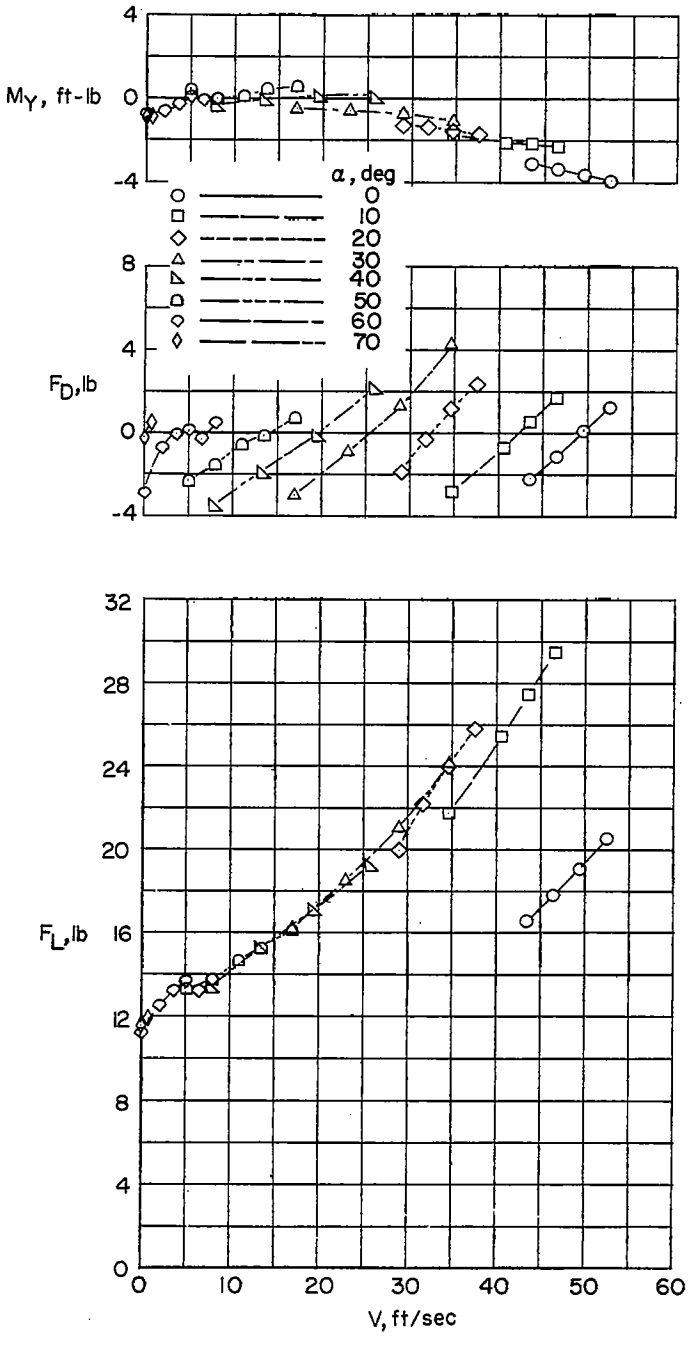

(f) $\delta_f = 40^\circ$; slat on.

Figure 4.- Continued.

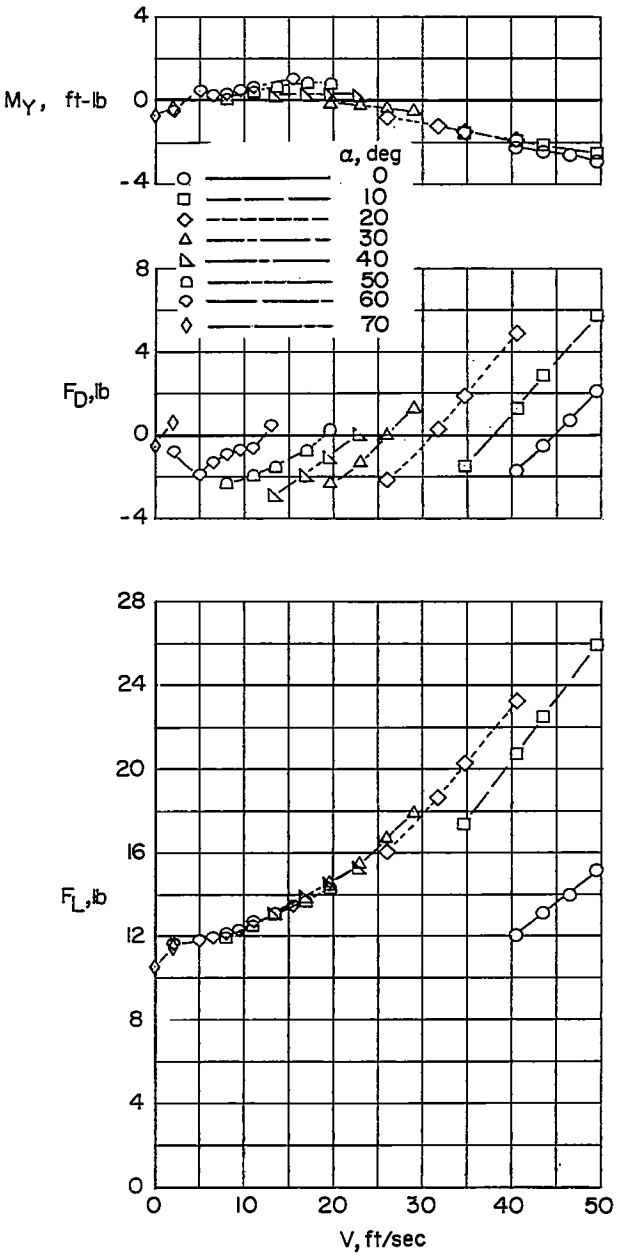

(g) $\delta_f = 60^\circ$; slat off.

Figure 4.- Continued.

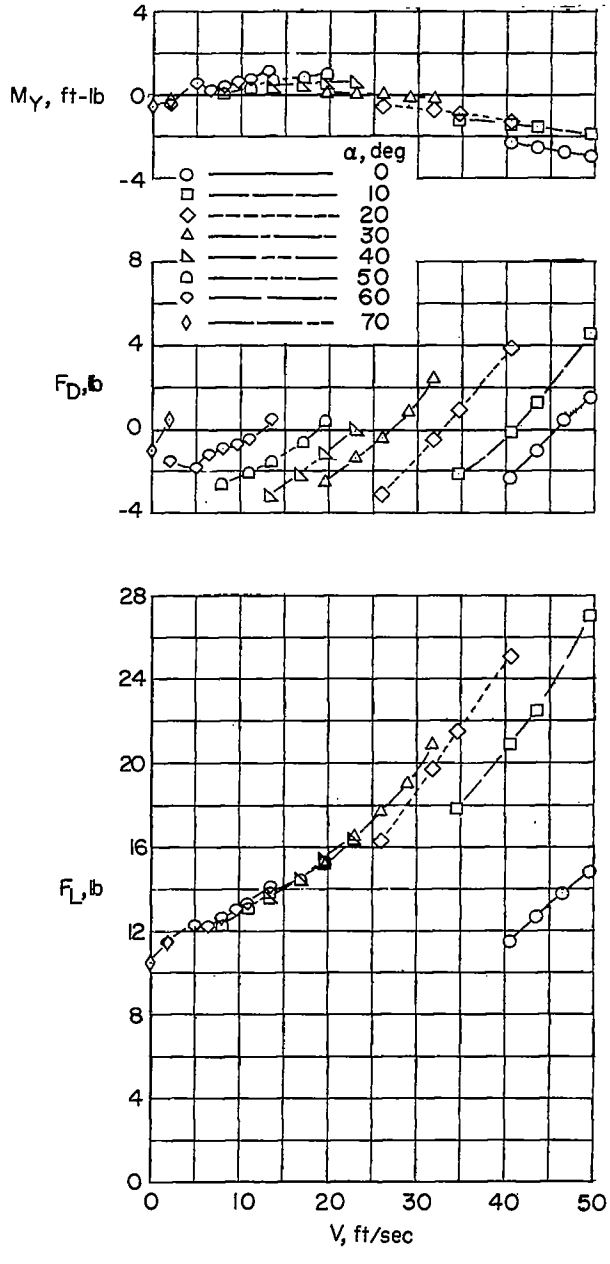

(h) $\delta_f = 60^\circ$; slat on.

Figure 4.- Concluded.

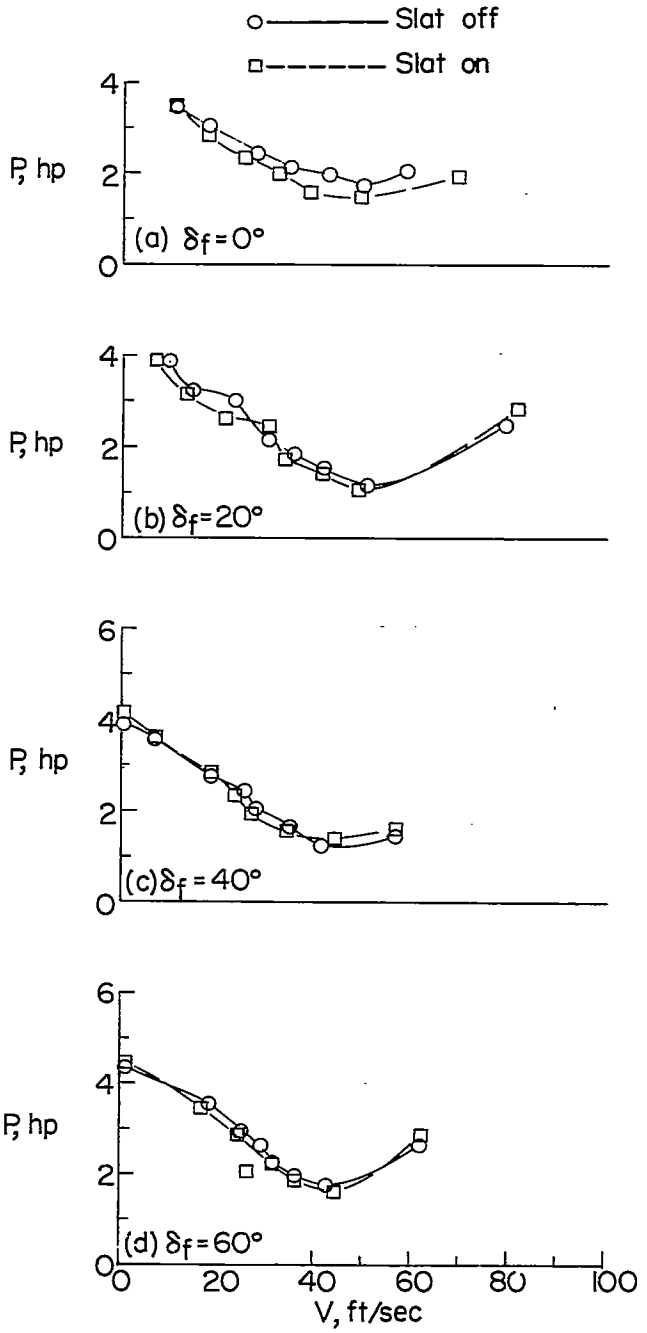

Figure 5.- Power input to model motor required through transition scaled up for a constant lift of 25 pounds. Drag = 0.

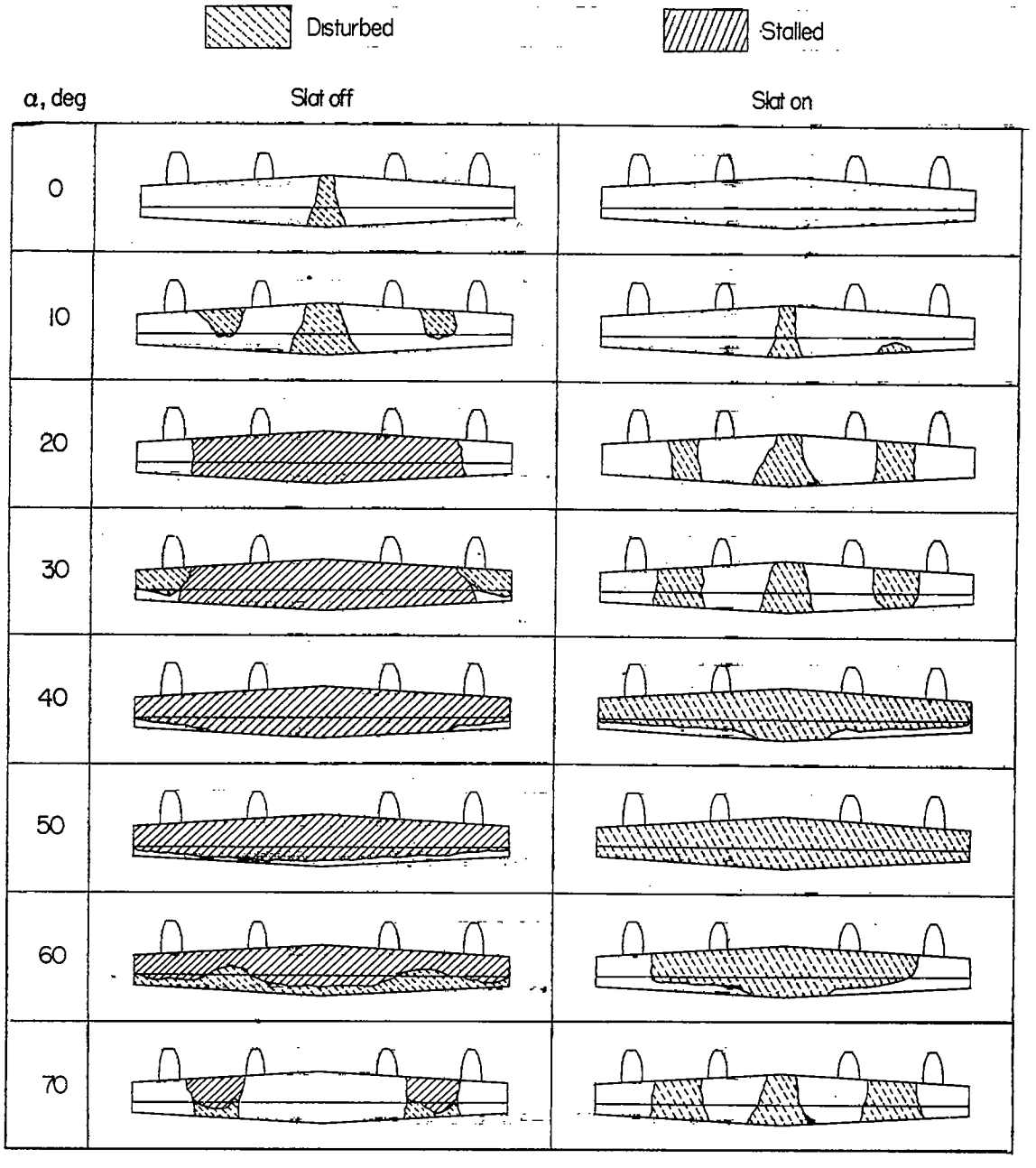

(a) $\delta_f = 0°$.

Figure 6.- Stall diagrams. Propeller position, upper forward; drag = 0.

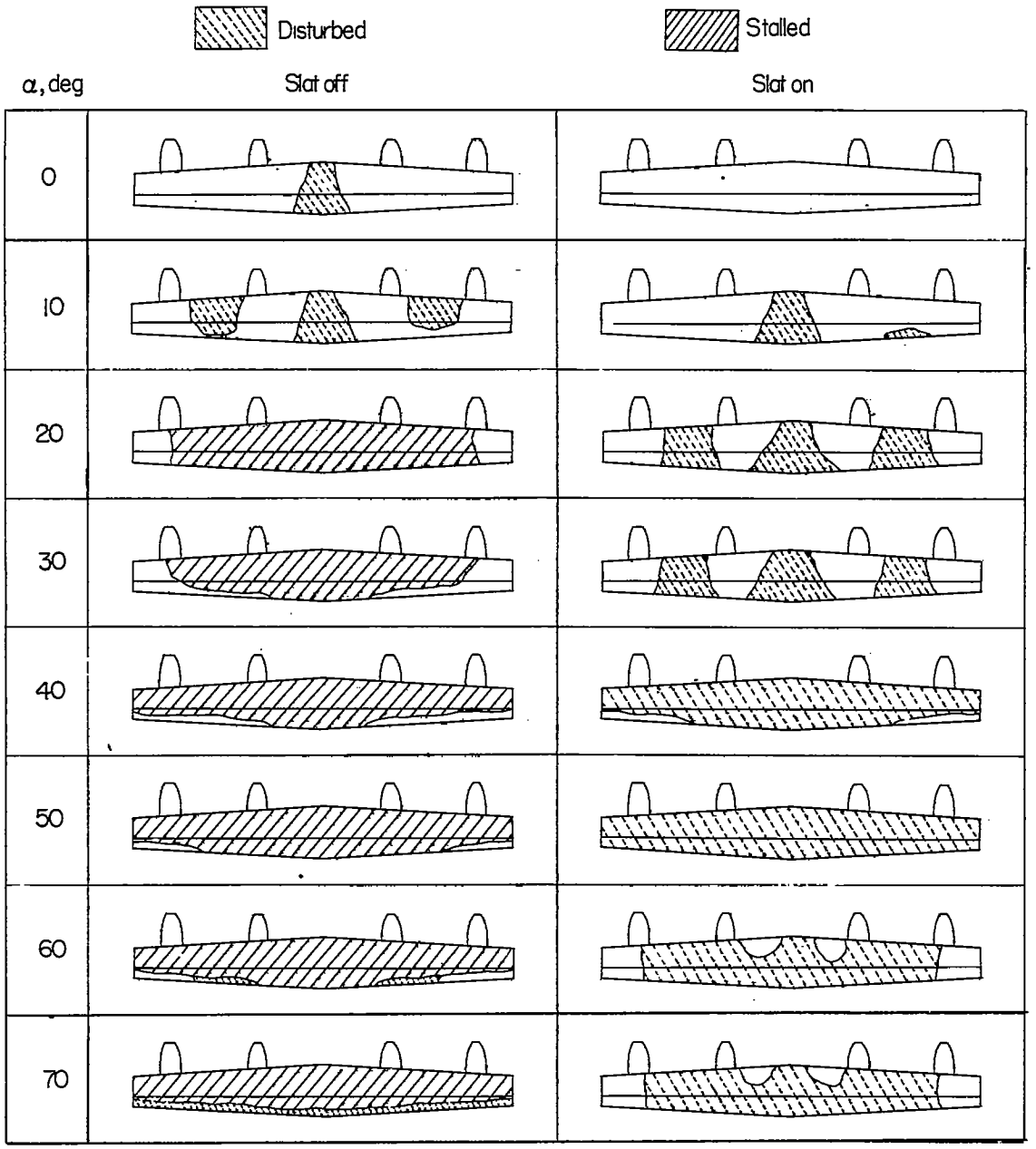

(b) $\delta_f = 20^\circ$.

Figure 6.- Continued.

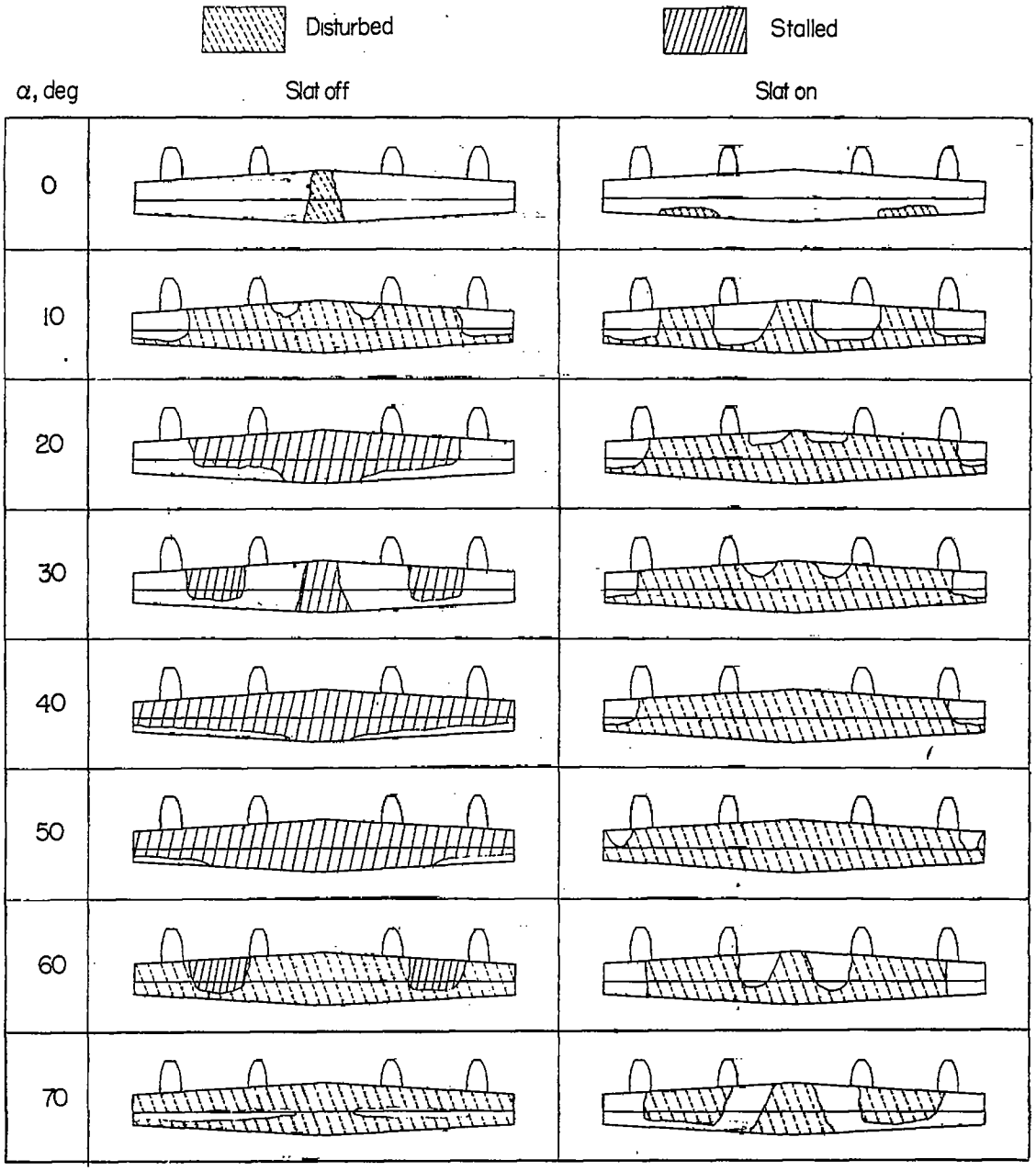

(c) $\delta_f = 40°$.

Figure 6.- Continued.

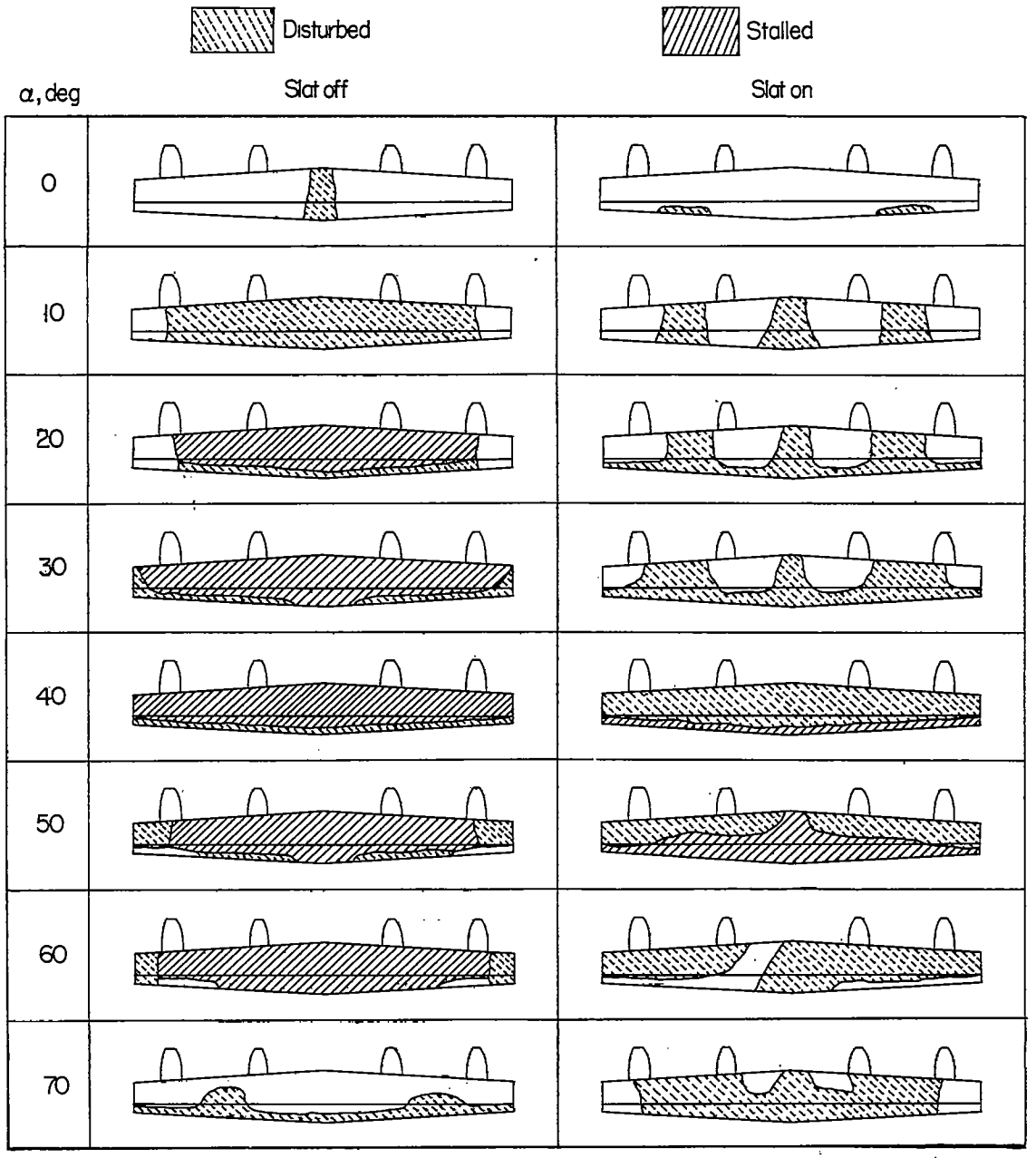

(d) $\delta_f = 60^\circ$.

Figure 6.- Concluded.

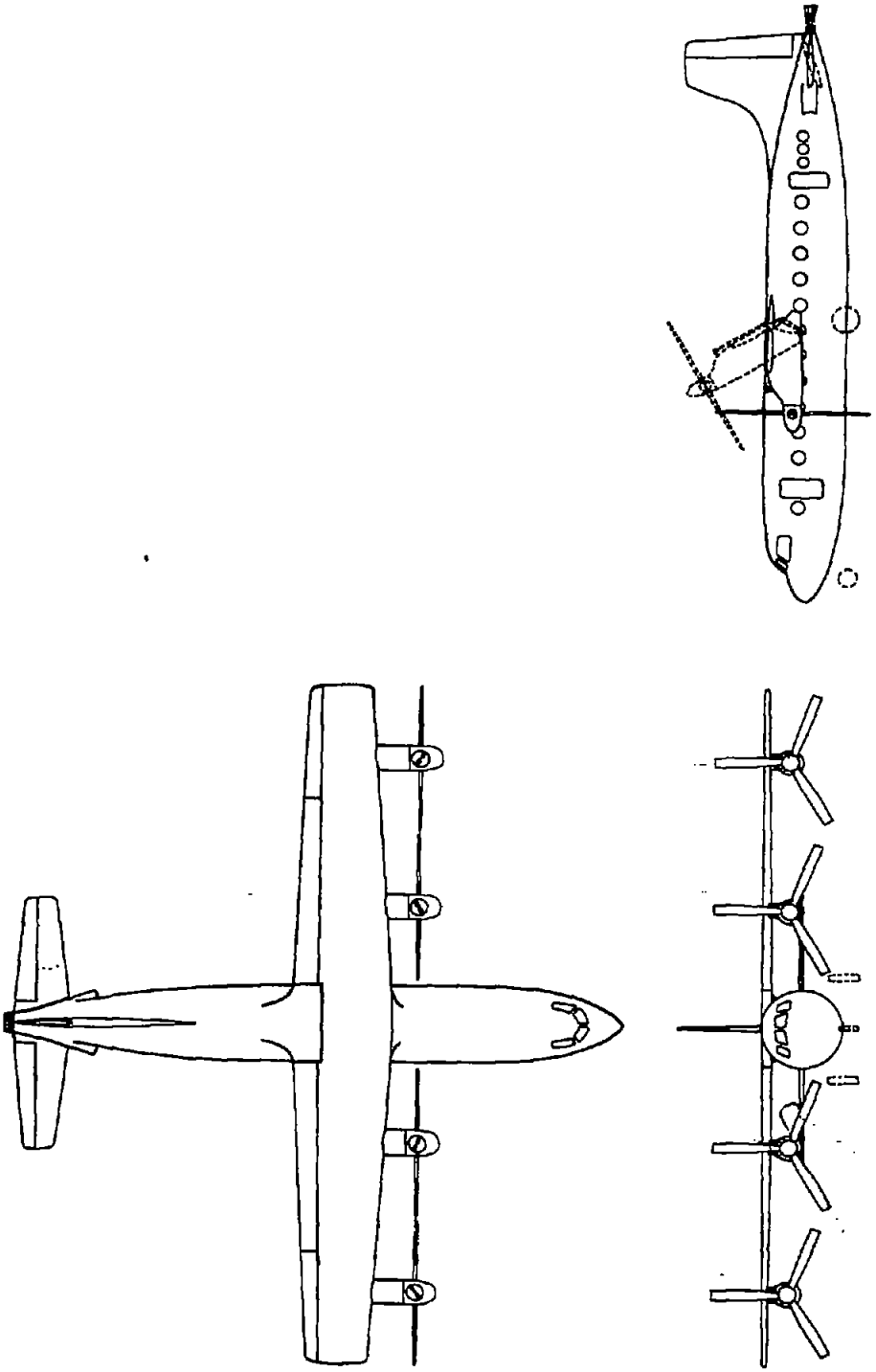

Figure 7.- Hypothetical vertical take-off airplane taken from reference 3.

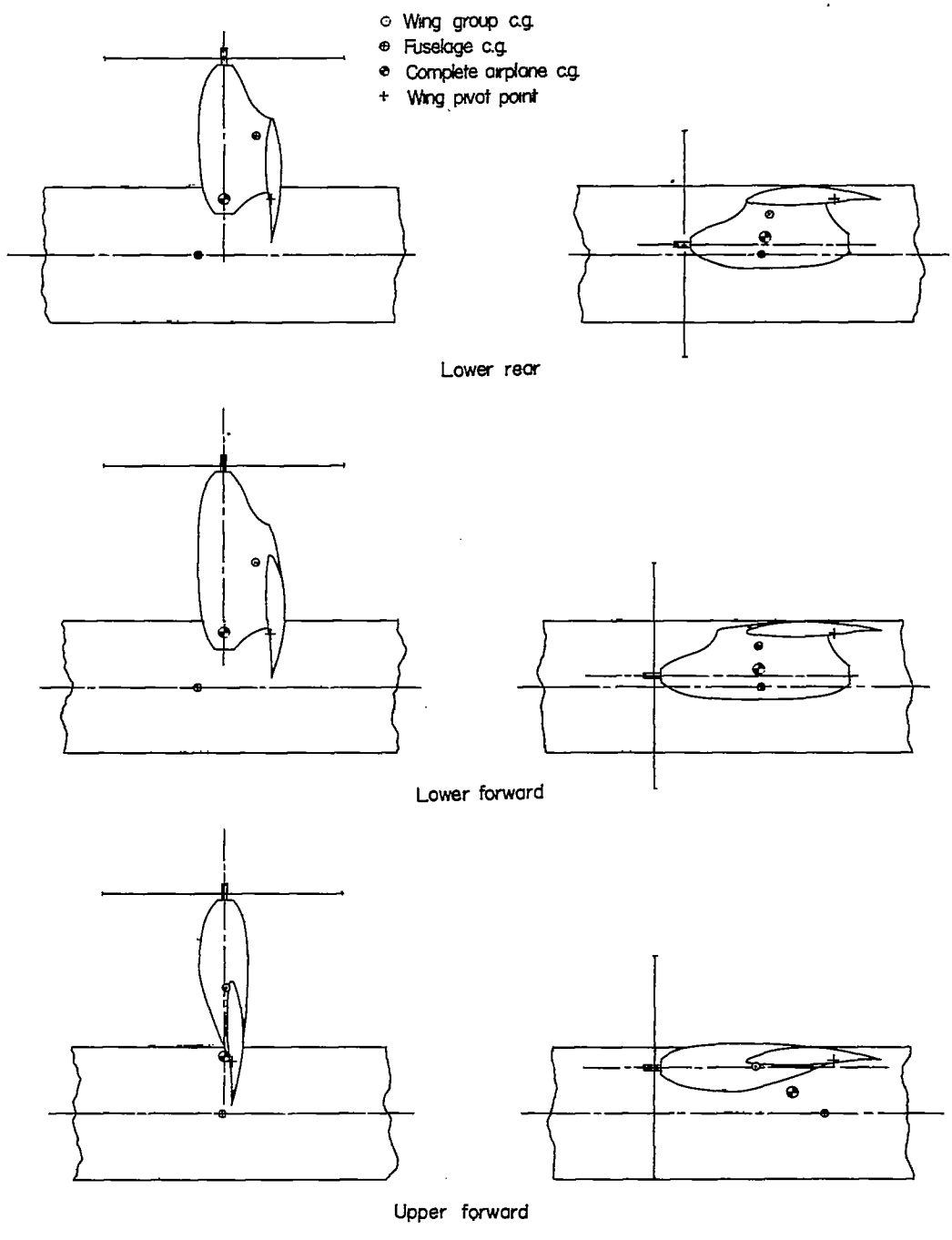

Figure 8.- Assumed center of gravity positions for various nacelle arrangements of hypothetical airplane.

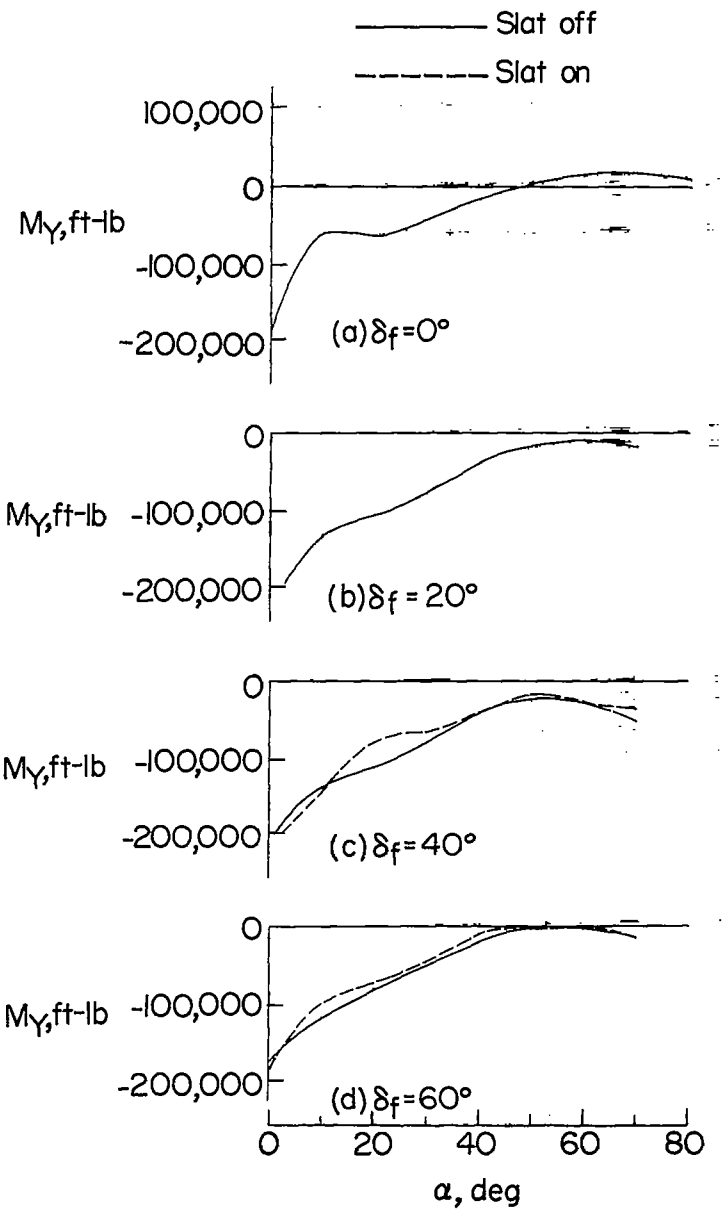

(a) Lower rear propeller position.

Figure 9.- Variation of pitching moment of wing-propeller combination with angle of attack for the hypothetical airplane shown in figure 7 - taken for case of zero drag, zero fuselage angle of attack, and for the relative centers of gravity of the fuselage and wing groups shown in figure 8.

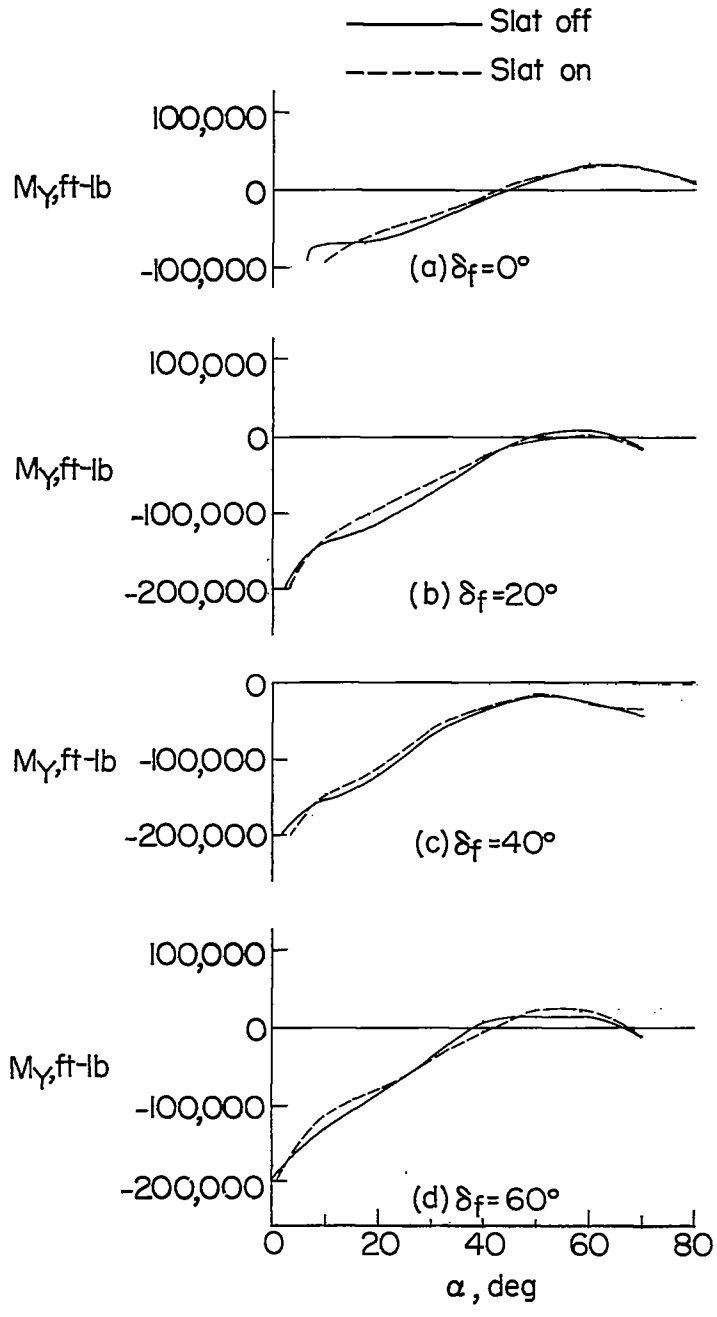

(b) Lower forward propeller position.

Figure 9.- Continued.

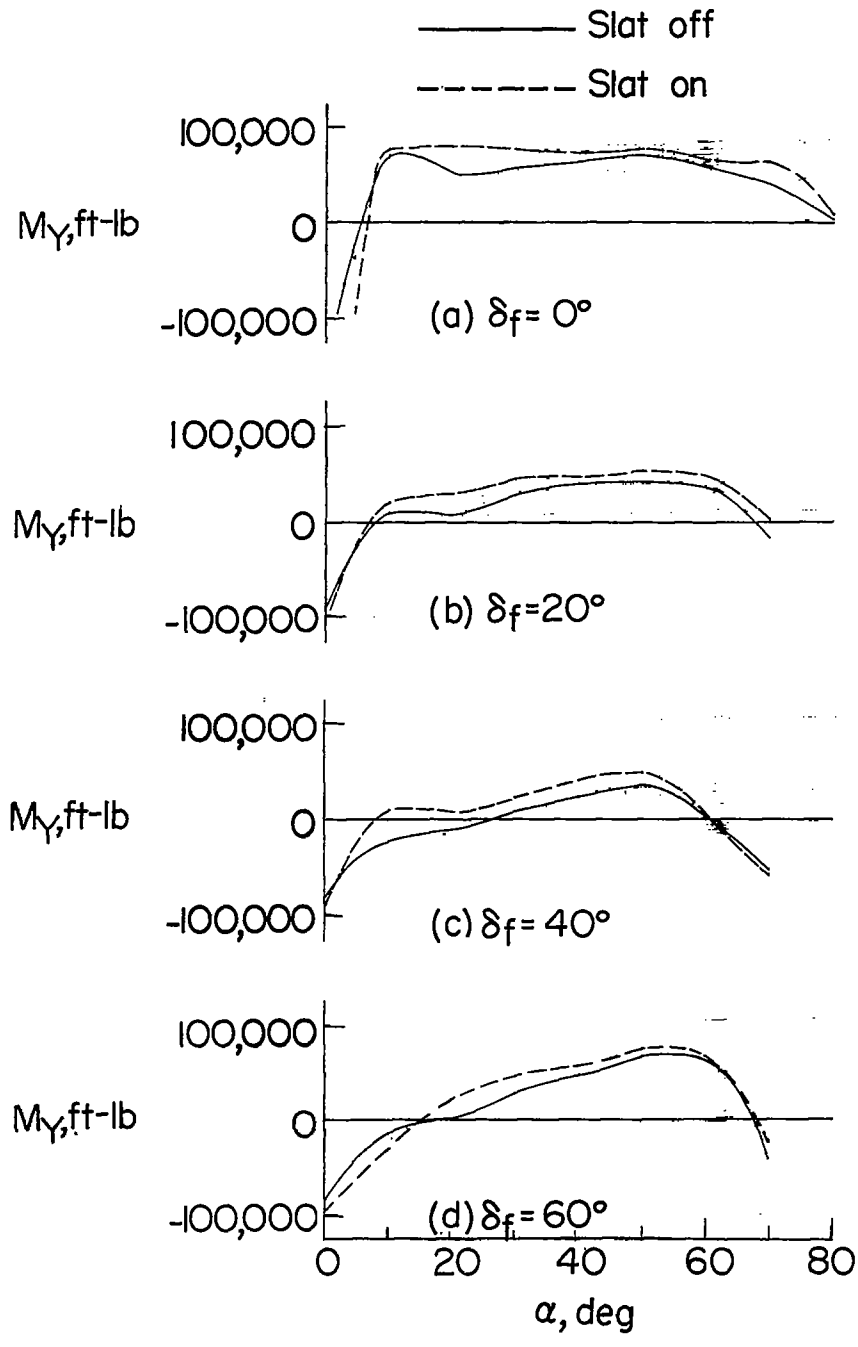

(c) Upper forward propeller position.

Figure 9.- Concluded.

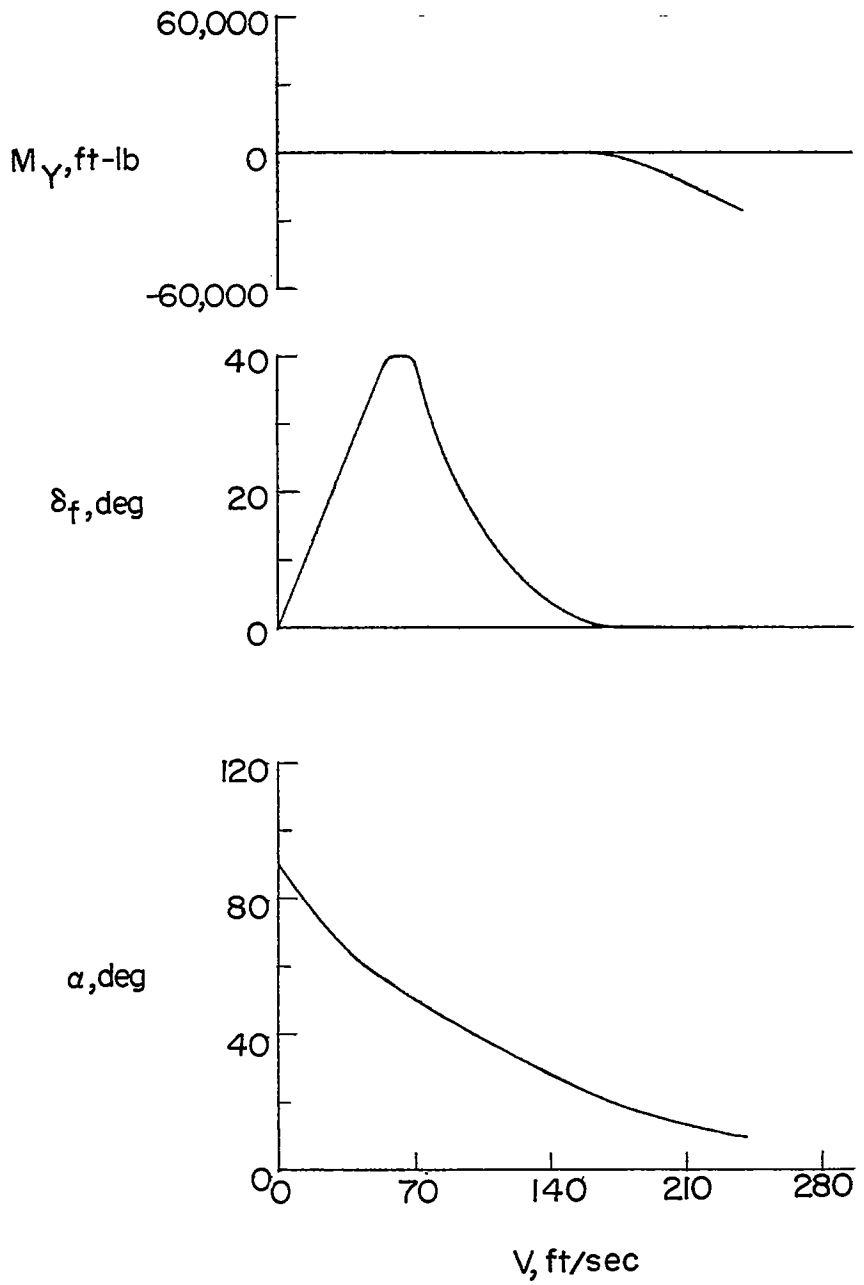

Figure 10.- Variation of pitching moment, flap deflection, and wing angle of attack of wing-propeller combination with velocity for the hypothetical airplane of figure 7 with an optimumized propeller location and variation of flap deflection with angle of attack.